Atlantic Geoscience
Journal of the Atlantic Geoscience Society

Geochronology and geochemistry of zircon from Early to Middle Devonian granitic and felsic volcanic rocks from the Cashes Ledge igneous suite, central Gulf of Maine, USA

Géochronologie et géochimie du zircon de roches volcaniques et plutoniques granitiques du Dévonien précoce à moyen provenant de la suite ignée Cashes Ledge, dans le centre du golfe du Maine, États-Unis

Yvette D. Kuiper, Sandra M. Barr, James L. Crowley and A. Kate Souders

Volume 59, 2023

URI: https://id.erudit.org/iderudit/1106341ar
DOI: https://doi.org/10.4138/atlgeo.2023.005

See table of contents

Publisher(s)

Atlantic Geoscience Society

ISSN

2564-2987 (digital)

Explore this journal

Cite this article

Kuiper, Y., Barr, S., Crowley, J. & Souders, A. (2023). Geochronology and geochemistry of zircon from Early to Middle Devonian granitic and felsic volcanic rocks from the Cashes Ledge igneous suite, central Gulf of Maine, USA. *Atlantic Geoscience*, *59*, 109–121. https://doi.org/10.4138/atlgeo.2023.005

Article abstract

New zircon U–Pb, trace element, and Lu–Hf laser ablation inductively coupled mass spectrometry (LA-ICP-MS) data are presented for five Early to Middle Devonian granitic and felsic volcanic rocks from the Cashes Ledge igneous suite, central Gulf of Maine, USA. These samples were previously analyzed by U–Pb LA-ICP-MS and whole-rock geochemical methods and the new data generally corroborate the earlier results. Coarse-grained alkali-feldspar granite from northwest of the Fundy magnetic anomaly, the interpreted fault boundary in the offshore between Gondwanan microcontinents Ganderia to the northwest and Avalonia to the southeast, yielded a crystallization age of 414 ± 2 Ma. Southeast of the inferred fault, crystallization ages are 385 ± 3 Ma and 386 ± 3 Ma for two crystal tuff samples near the fault, 403 ± 3 Ma for an alkali-feldspar granite ~50 km southeast of the fault, and 399 ± 5 Ma for syenogranite ~25 km southeast of the fault, which also yielded inherited grains at ~1.3 Ga and between 613 ± 15 Ma and 558 ± 9 Ma. Lu–Hf LA-ICP-MS data for zircon retaining igneous crystallization ages have εHf(t) between 2.9 and 13.1 and model ages based on felsic sources between 0.52 and 1.04 Ga, reflecting a mix of late Mesoproterozoic (Avalonian?) basement and primitive melt, possibly in an extensional setting. Zircon Nb/Hf ratios generally greater than 0.001 indicate a predominately within-plate/anorogenic/rift setting, consistent with their whole-rock chemistry. U/Yb-Nb/Yb and U/Yb-Hf tectonic setting discrimination diagrams show ocean island to continental arc signatures, with a stronger continental arc signature for the syenogranite. Most zircon grains have Eu/Eu* values less than 0.1, indicating a crustal thickness of ~30 km or less at the time of their crystallization.

Geochronology and geochemistry of zircon from Early to Middle Devonian granitic and felsic volcanic rocks from the Cashes Ledge igneous suite, central Gulf of Maine, USA

Yvette D. Kuiper[1], Sandra M. Barr[2], James L. Crowley[3], and A. Kate Souders[4]

1. Department of Geology and Geological Engineering, Colorado School of Mines, Golden, Colorado 80401, USA
2. Department of Earth and Environmental Science, Acadia University; Wolfville, Nova Scotia B4P 2R6, Canada
3. Department of Geosciences, Boise State University, Boise, Idaho 83725-1535, USA
4. U.S. Geological Survey, Geology, Geophysics, and Geochemistry Science Center, Denver, 80225 Colorado, USA
Corresponding author <ykuiper@mines.edu>

Date received: 27 March 2023 ¶ Date accepted: 6 June 2023

ABSTRACT

New zircon U–Pb, trace element, and Lu–Hf laser ablation inductively coupled mass spectrometry (LA-ICP-MS) data are presented for five Early to Middle Devonian granitic and felsic volcanic rocks from the Cashes Ledge igneous suite, central Gulf of Maine, USA. These samples were previously analyzed by U–Pb LA-ICP-MS and whole-rock geochemical methods and the new data generally corroborate the earlier results. Coarse-grained alkali-feldspar granite from northwest of the Fundy magnetic anomaly, the interpreted fault boundary in the offshore between Gondwanan microcontinents Ganderia to the northwest and Avalonia to the southeast, yielded a crystallization age of 414 ± 2 Ma. Southeast of the inferred fault, crystallization ages are 385 ± 3 Ma and 386 ± 3 Ma for two crystal tuff samples near the fault, 403 ± 3 Ma for an alkali-feldspar granite ~50 km southeast of the fault, and 399 ± 5 Ma for syenogranite ~25 km southeast of the fault, which also yielded inherited grains at ~1.3 Ga and between 613 ± 15 Ma and 558 ± 9 Ma. Lu–Hf LA-ICP-MS data for zircon retaining igneous crystallization ages have $\varepsilon_{Hf(t)}$ between 2.9 and 13.1 and model ages based on felsic sources between 0.52 and 1.04 Ga, reflecting a mix of late Mesoproterozoic (Avalonian?) basement and primitive melt, possibly in an extensional setting. Zircon Nb/Hf ratios generally greater than 0.001 indicate a predominately within-plate/anorogenic/rift setting, consistent with their whole-rock chemistry. U/Yb-Nb/Yb and U/Yb-Hf tectonic setting discrimination diagrams show ocean island to continental arc signatures, with a stronger continental arc signature for the syenogranite. Most zircon grains have Eu/Eu* values less than 0.1, indicating a crustal thickness of ~30 km or less at the time of their crystallization.

RÉSUMÉ

De nouvelles données de datation U–Pb sur zircon, d'analyse d'éléments traces et de spectrométrie de masse à plasma inductif et ablation par laser (LA-ICP-MS) à des fins de datation par le Lu–Hf sont présentées par rapport à cinq roches granitiques et volcanofelsiques du Dévonien précoce à moyen provenant de la suite ignée Cashes Ledge, dans le centre du golfe du Maine, aux États-Unis. Les échantillons en question avaient précédemment été analysés par les méthodes de l'étude géochimique sur roche totale et LA-ICP-MS de datation U–Pb, et les nouvelles données corroborent de façon générale les résultats antérieurs. Le granite alcalo-feldspathique à gros grains de l'anomalie magnétique du nord-ouest de Fundy, limite interprétée de la faille au large entre les microcontinents gondwaniens de Ganderia au nord-ouest et d'Avalonia au sud-est, a accusé un âge de cristallisation de 414 ± 2 Ma. Au sud-est de la faille inférée, les âges de la cristallisation sont de 385 ± 3 Ma et 386 ± 3 Ma dans le cas de deux échantillons de tuf cristallin près de la faille, 403 ± 3 Ma dans le cas d'un granite alcalo-feldspathique à une cinquantaine de kilomètres au sud-est de la faille, et 399 ± 5 Ma dans le cas du syénogranite à environ 25 km au sud-est de la faille, qui a aussi livré des grains hérités d'environ 1,3 Ga et d'entre 613 ± 15 Ma et 558 ± 9 Ma. Les données LA-ICP-MS de datation par le Lu–Hf du zircon révélant les âges de la cristallisation ignée situent les âges entre 2,9 et 13,1 s'inspirant de sources felsiques entre 0,52 et 1,04 Ga, ce qui témoigne d'un mélange d'une fusion primitive et d'une fusion du socle tardive mésoprotérozoïque (avalonienne?), possiblement dans un milieu d'extension. Les rapports Nb/Hf sur zircon généralement supérieurs à 0,001 signalent un milieu intraplaque/anorogénique/de rift correspondant à la composition chimique de sa roche totale. Des schémas de discrimination des milieux tectoniques U/Yb-Nb/Yb et U/Yb-Hf affichent des signatures d'îles océaniques à et des arcs continentaux dans le cas du syénogranite. La majorité des grains de zircon présentent des concentrations d'Eu/Eu* de moins de 0,1 témoignant d'une épaisseur de la croûte d'une trentaine de kilomètres ou moins au moment de leur cristallisation.

[*Traduit par la redaction*]

doi:10.4138/atlgeo.2023.005

INTRODUCTION

We obtained zircon U–Pb, trace element, and Lu–Hf laser ablation inductively coupled mass spectrometry (LA-ICP-MS) data to investigate the nature, tectonic setting, and basement of five Early to Middle Devonian granitic and felsic tuff samples from the central Gulf of Maine (Fig. 1). The purpose was to better constrain terrane boundaries in the Gulf of Maine, in the context of onshore geology. The samples are part of a larger suite collected in 1971–1972 from seafloor outcrops in the central Gulf of Maine using the submersible Alvin (Ballard 1974). This collection had been studied previously by Hermes *et al.* (1978) and Barr *et al.* (2011), who gave them the collective name Cashes Ledge igneous suite. The earlier work had included petrographic and whole-rock major and trace element analyses and Barr *et al.* (2011) had also reported U–Pb LA-ICP-MS zircon ages from the same five samples used in this study.

Our study was undertaken to enhance this earlier work through additional U–Pb LA-ICP-MS analysis of zircon, as well as zircon trace element and Lu–Hf isotopic analyses. We specifically targeted zircon cores in the five samples previously analyzed to search for evidence of inheritance, with the goal of obtaining information about the age and

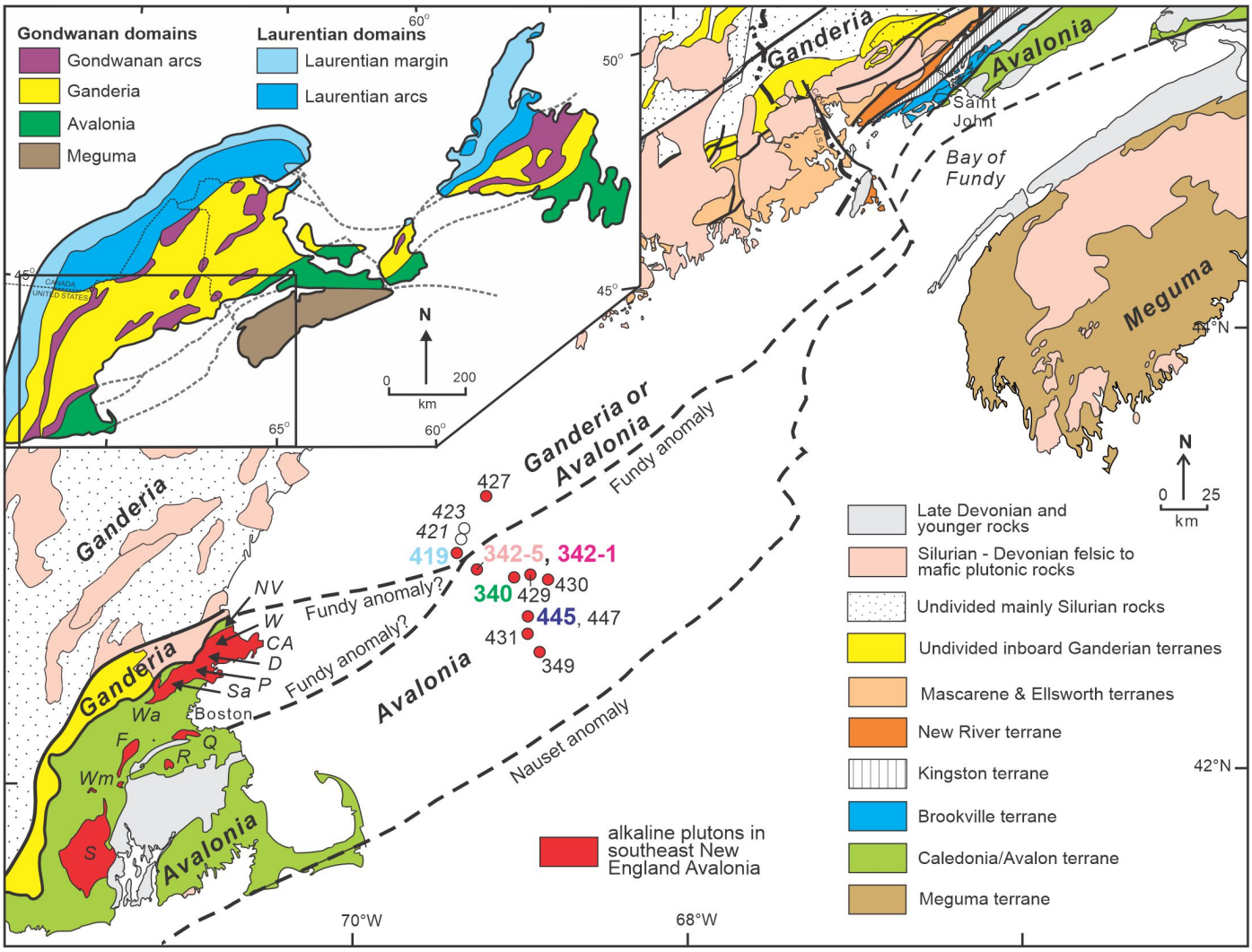

Figure 1. Locations of samples in the Gulf of Maine and simplified geology after Hibbard *et al.* (2006), Barr *et al.* (2011) and Thompson *et al.* (2018). Sample sites are indicated by numbers following Ballard (1974). Samples from sites 421 and 423 were studied by Hermes *et al.* (1978). All other samples were described and analyzed using whole-rock major and trace geochemistry by Barr *et al.* (2011). Samples 419, 340, 445, 342-1, and 342-5 were analyzed by U–Pb LA-ICP-MS methods by Barr *et al.* (2011) and in this study. Color coding corresponds to those used in Figures 2, 3, and 5. Inset map shows components of the northern Appalachian orogen after Hibbard *et al.* (2006). Approximate locations of alkaline/peralkaline rocks in Avalonia in southeastern New England are indicated as follows: CA, Cape Ann (~426 Ma); D, Danvers (~444 Ma); F, Franklin (~417 Ma); P, Peabody (~378 Ma); Q, Quincy (~412 Ma); R, Rattlesnake (~378 Ma); S, Scituate (~370 Ma); Sa, Salem gabbro/diorite (~392 Ma); W, Wenham (~378 and ~395 Ma); Wa, Waltham gabbro/diorite (~378 Ma); Wm, Wamsutta rhyolite (~373 Ma).

characteristics of the continental basement under the Gulf of Maine. Trace element geochemistry was included during U–Pb analysis to enable calculation of the temperature of zircon crystallization and estimation of crustal thickness during crystallization, and to interpret the tectonic setting.

The analyzed samples are from both sides of the Fundy magnetic anomaly, which has been interpreted to mark the boundary in the offshore between the Gondwana-derived microcontinents of Ganderia to the northwest and Avalonia to the southeast (Hibbard *et al.* 2006). Ganderia has been interpreted to have rifted from the Amazonian part of the supercontinent Gondwana in the Cambrian and accreted to Laurentia during the Late Ordovician and Silurian Salinic orogeny (e.g., Nance *et al.* 2008; Pollock *et al.* 2012; van Staal *et al.* 2009, 2021b; Kay *et al.* 2017). Avalonia may have Amazonian and/or Baltican and/or West African origins (e.g., Nance *et al.* 2008; Pollock *et al.* 2012; van Staal *et al.* 2021a; Severson *et al.* 2022; Thompson *et al.* 2022; Murphy *et al.* 2023) and accreted to Laurentia during the latest Silurian to Middle Devonian Acadian orogeny (e.g., Skehan and Rast 1990; Nance *et al.* 2008; van Staal *et al.* 2009, 2021a, b).

The Fundy magnetic anomaly is a ~10 km wide aeromagnetic high, and part of a series of short-wavelength, high amplitude linear magnetic anomalies to the northwest (Hutchinson *et al.* 1988). The southeastern part of the Fundy magnetic anomaly coincides with the top of a southeasterly dipping seismic reflector, interpreted as the Fundy Fault. It separates a zone of southeasterly dipping seismic reflectors to the northwest from predominantly subhorizontal reflections to the southeast (Hutchinson *et al.* 1988). The results of Barr *et al.* (2011) confirmed the alkalic characteristics of the Cashes Ledge igneous suite that had been suggested by Hermes *et al.* (1978) based on petrography and whole-rock geochemistry. However, the U–Pb LA-ICP-MS zircon data demonstrated that their ages are Early to Middle Devonian (Barr *et al.* 2011), and hence younger than the Ordovician U–Pb zircon ID-TIMS ages of Hermes *et al.* (1978). The nature of the basement or host rocks in the context of onshore terranes remained unclear.

PREVIOUS WORK

Barr *et al.* (2011) obtained 13 samples from the Cashes Ledge igneous suite from the archives at Woods Hole Oceanographic Institute, representing 10 of the 12 locations sampled by Ballard (1974) and studied by Hermes *et al.* (1978). Samples from two sites, 421 and 423, were no longer available. Two samples were used from site 445, three from site 342, and one sample from each of the other eight sites (Fig. 1). The samples are plutonic except for one arkosic sandstone and two felsic tuff samples from site 342. In addition to petrographic study of all the samples, Barr *et al.* (2011) did whole-rock major- and trace-element analyses of the ten granitic and two felsic tuff samples, and U–Pb laser ablation inductively coupled mass spectrometry (LA-ICP-MS) dating of zircon grains from the two felsic tuff samples and three of the granitic samples.

Major and trace element analyses indicated that most of the 12 igneous samples are alkaline to weakly peralkaline based on agpaitic index (Barr *et al.* 2011; cf. Hermes *et al.* 1978). The two volcanic samples from location 342 yielded low Na and K relative to Al, and hence plot in the calc-alkaline field. However, the groundmass in these rocks is fine grained and altered, and the Na and K data may not reflect their original igneous compositions. They demonstrated that the samples are generally alkaline to slightly peralkaline, with iron-rich mafic minerals, high concentrations of SiO_2, Y, Zr, Nb, and REE, strong negative Eu anomalies, and ε_{Nd} values from the five dated samples range from +3.7 to –0.5 (Barr *et al.* 2011).

Alkali-feldspar granite sample ALV419-1-2 is from ~30 km NW of the Fundy magnetic anomaly (Fig. 1) and 40 km from the inferred trace of the Fundy Fault (cf. Hutchinson *et al.* 1988), and hence was interpreted as emplaced in Ganderian crust (Barr *et al.* 2011). It yielded a U–Pb LA-ICP-MS zircon crystallization age of 414.9 ± 1.1 Ma (Barr *et al.* 2011). The remaining four samples were collected SE of the Fundy anomaly in crust interpreted to be in Avalonia. Felsic tuff samples ALV342-1-1 and ALV342-5-3 nearest the Fundy anomaly yielded crystallization ages of 384.4 ± 2.3 Ma and 383.9 ± 1.6 Ma (Barr *et al.* 2011). Other reported crystallization ages were 399.7 ± 1.5 Ma for alkali-feldspar granite ALV445-1-2 and 407.0 ± 1.9 Ma for syenogranite sample ALV340-1-7A (Barr *et al.* 2011). The samples resemble those in a belt of rocks of similar Silurian–Devonian age in the central part of Avalonia in southeastern New England that likely formed in an extensional setting linked to subduction and subsequent transcurrent motions between various Gondwanan terranes (Barr *et al.* 2011; Thompson *et al.* 2018).

DESCRIPTIONS OF DATED SAMPLES

Zircon separates for the five samples dated by Barr *et al.* (2011) were used in this study. Based on descriptions from Barr *et al.* (2011), tuffaceous samples ALV-342-1-1 and ALV-342-5-3 contain embayed quartz and highly sericitized feldspar crystals in a mainly cryptocrystalline quartzofeldspathic groundmass. Relict eutaxitic banding and possible lithophysae are visible in sample ALV-342-1-1, whereas sample ALV-342-5-3 is sheared and more altered with no relict igneous textures preserved. Sample ALV-419-1-2 is coarse-grained alkali-feldspar granite consisting mostly of perthitic K-feldspar and quartz, with less than 3% clinopyroxene and amphibole. The pyroxene is high in Fe and Na, and of aegirine-augite composition. The amphibole forms mostly large grains with blue-green pleochroism and sodic–calcic and Fe-rich compositions, and minor fibrous pleochroic blue riebeckite is also present. Sample ALV-445-1-5 is a similar alkali-feldspar granite, but contains minor biotite, as well as pyroxene and amphibole. Pyroxene analyses from sample ALV-445-1-5 are high in Fe and Na, but less than the

pyroxene in sample ALV-419-1-2. Amphibole analyses are also high in Fe but lack significant amounts of Ca or Na and are classified as grunerite. Biotite is also Fe-rich and has relatively low Al. Sample ALV-340-1-7A is medium- to coarse-grained syenogranite with separate crystals of K-feldspar and plagioclase and patches of coarse granophyre. The feldspars are intensively altered to sericite, and the rock is brecciated. Minor ferromagnesian minerals are altered to iron oxide.

METHODS

Zircon was separated using conventional crushing, grinding and wet shaking table methods, followed by heavy liquid and magnetic separation, at the Pacific Centre for Isotopic and Geochemical Research (Barr *et al.* 2011). For our study, U–Pb LA-ICP-MS analysis was carried out at Boise State University (see Appendix for detailed methods) on the zircon separates remaining from the study by Barr *et al.* (2011). Prior to analysis, zircon grains were annealed at 900˚C for 60 hours in a muffle furnace (cf. Allen and Campbell 2012), and mounted in epoxy and polished until their centers were exposed. Cathodoluminescence (CL) images were obtained with a JEOL JSM-300 scanning electron microscope and Gatan MiniCL. Lu–Hf LA-ICP-MS analysis was carried out at the USGS – Denver Federal Center on zircon grains used for U–Pb analysis, except for 32 grains from sample ALV-340-1-7A, on which U–Pb analysis was carried out subse-quently in an unsuccessful attempt to find more pre-Ediaca-ran zircon cores. Detailed Lu–Hf methods are outlined in the Appendix.

RESULTS

Ages and Lu–Hf data are summarized in Table 1, and zircon characteristics and geochemistry are further described below. We use shortened sample numbers for simplicity, as shown in Table 1. Interpretation of igneous crystallization ages from LA-ICP-MS dates is difficult in these type of samples with dates that are not equivalent (probability of fit >0.05), likely due to inherited grains that yield dates that are older than crystallization and domains that suffered Pb loss that yield younger dates. In some samples, these older and younger dates are obvious and thus are not included in the weighted mean calculations. However, in other samples they are not obvious. Our calculations include the maximum number of dates that are equivalent (probability of fit >0.05), starting at the young end of the age spectrum, aside from dates that are considerably younger and thus likely are in domains that suffered considerable Pb loss.

Lu–Hf depleted mantle model ages (T_{DM}) were calculated assuming both mafic and felsic sources (Table 1). Those based on felsic sources are used for further interpretation, because Hf isotope trajectories based on ε_{Hf}/age ratios for both Avalonia and Ganderia in the Canadian Appalachians show mostly $^{176}Lu/^{177}Hf$ ratios of 0.010–0.015, corresponding to more felsic sources (Pollock *et al.* 2022). Furthermore, published Sm–Nd model ages for these same samples are 0.73–1.0 Ga (Barr *et al.* 2011). For igneous rocks in Avalonia in the Caledonia terrane in New Brunswick, Canada, they are 0.78–1.31 Ga (Samson *et al.* 2000), and in the Antigonish Highlands of Nova Scotia, Canada, model ages are ~0.65–1.15 Ga (Murphy and Nance 2002; White *et al.* 2021). In the samples analyzed in this study, zircon Lu–Hf T_{DM} of 0.52–1.04 Ga based on felsic sources are more consistent with these Sm–Nd model ages than the 0.59–1.49 Ga based on mafic sources. In Avalonia in southeastern New England, USA, Sm–Nd model ages of Ediacaran granites are ~0.96–1.15 Ga, but range up to ~2.2 Ga (Thompson *et al.* 2012) and zircon Lu–Hf model ages based on felsic sources are ~1.0–1.3 Ga (Thompson *et al.* 2022).

Zircon grain CL images are presented in Supplementary Date File S1. Zircon LA-ICP-MS data for U–Pb and Lu–Hf are presented in Supplementary Data tables S2-6, and S7, respectively (URL links are in Appendix).

Table 1. Summary of previous and new U–Pb and Lu–Hf results.

sample number	short name	rock type; age (Ma) after Barr *et al* . (2011)	Age (Ma)	$\varepsilon_{Hf(t)}$	T_{DM} felsic (Ga)	T_{DM} mafic (Ga)
ALV-419-2-1	419	coarse-grained alkali- feldspar granite; 414.9 ± 1.1 Ma	414 ± 2	2.9–13.1	0.52–1.04	0.59–1.49
ALV-445-1-2	445	alkali-feldspar granite; 399.7 ± 1.5 Ma	403 ± 3	3.8–6.8	0.83–0.99	1.13–1.40
ALV-340-1-7A	340	syenogranite; 407.0 ± 3.9 Ma	399 ± 5 613 ± 15 to 554 ± 29 1281 ± 23	3.3–6.8 1.6–6.1 10	0.84–1.02 1.00–1.26 1.39	1.15–1.45 1.32–1.73 1.46
ALV-342-1-1A	342-1	crystal tuff; 384.4 ± 2.3 Ma	385 ± 3	4.5–8.0	0.75–0.94	1.02–1.33
ALV-342-5-3	342-5	crystal tuff (sheared/altered); 383.9 ± 1.6 Ma	386 ± 3	4.6–10.1	0.65–0.95	0.84–1.34

Sample 419 – coarse-grained alkali-feldspar granite

Zircon grains are generally euhedral with aspect ratios of 1:1.5 to 1:2 and show concentric and sector zoning. Although some grains show darker cores and lighter rims in CL (Supplementary Data File S1), zoning is continuous across these color differences, which are interpreted to reflect changes in melt composition and not separate growth events. Thirty-six grains yielded dates between 429 ± 15 Ma and 387 ± 11 Ma (Fig. 2a; Supplementary Data Table S2). A weighted mean date from 33 dates is 414 ± 2 Ma (mean square weighted deviation (MSWD) = 1.1, probability of fit (pof) = 0.27), interpreted as the igneous crystallization age. It is within error of the age of 414.9 ± 1.1 Ma reported by Barr *et al.* (2011). Two older dates are interpreted as being from inherited components. Grain 379 yielded the youngest date of 387 ± 11 Ma; it is brighter in CL than most other grains and is interpreted to have experienced Pb loss. It has a lower Lu/Hf ratio (0.007) than the other grains.

Most zircon grains show similar chemical characteristics, but Lu/Hf ratios generally plot in two groups with ratios <0.010 and 0.015–0.025 (Fig. 3i). The spot analyses of these groups correspond to CL-bright and CL-dark domains, respectively. Low Lu/Hf and CL-bright domains also correspond with low Nb/Ta and low REE (Figs. 3e, g). This sample has a higher REE content than the other samples (Figs. 3g, 4a). U/Yb-Nb/Yb and U/Yb-Hf tectonic discrimination diagrams (cf. Grimes *et al.* 2015) show weak continental arc

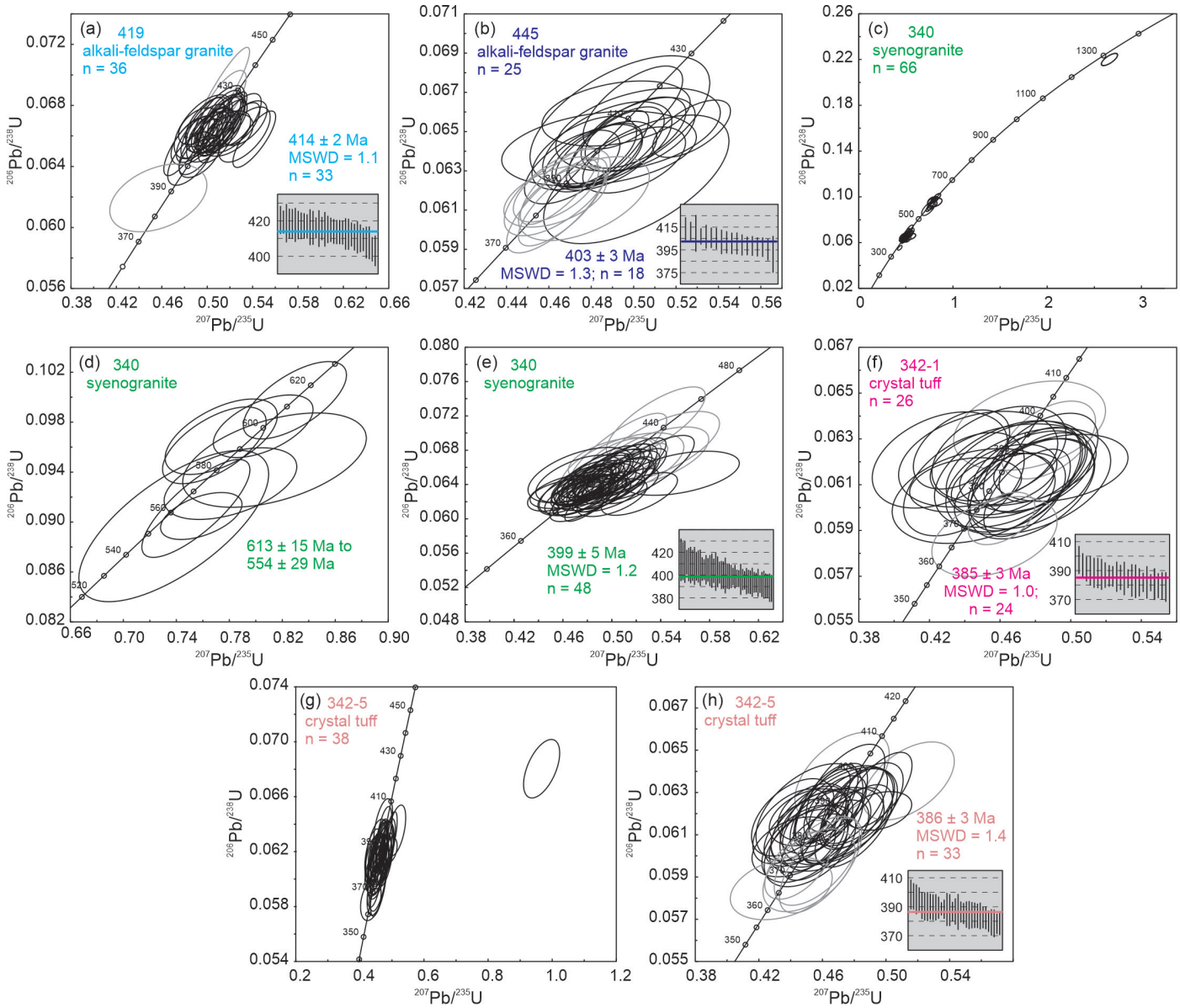

Figure 2. Wetherill Concordia diagrams showing U–Pb LA-ICP-MS geochronology data (Supplementary Data tables S2-S6). Weighted mean of $^{206}Pb/^{238}U$ ages of main age populations (black ellipses in the same diagrams) indicated. Data ellipses are 2σ. The mean squared weighted deviation (MSWD) are noted in each diagram.

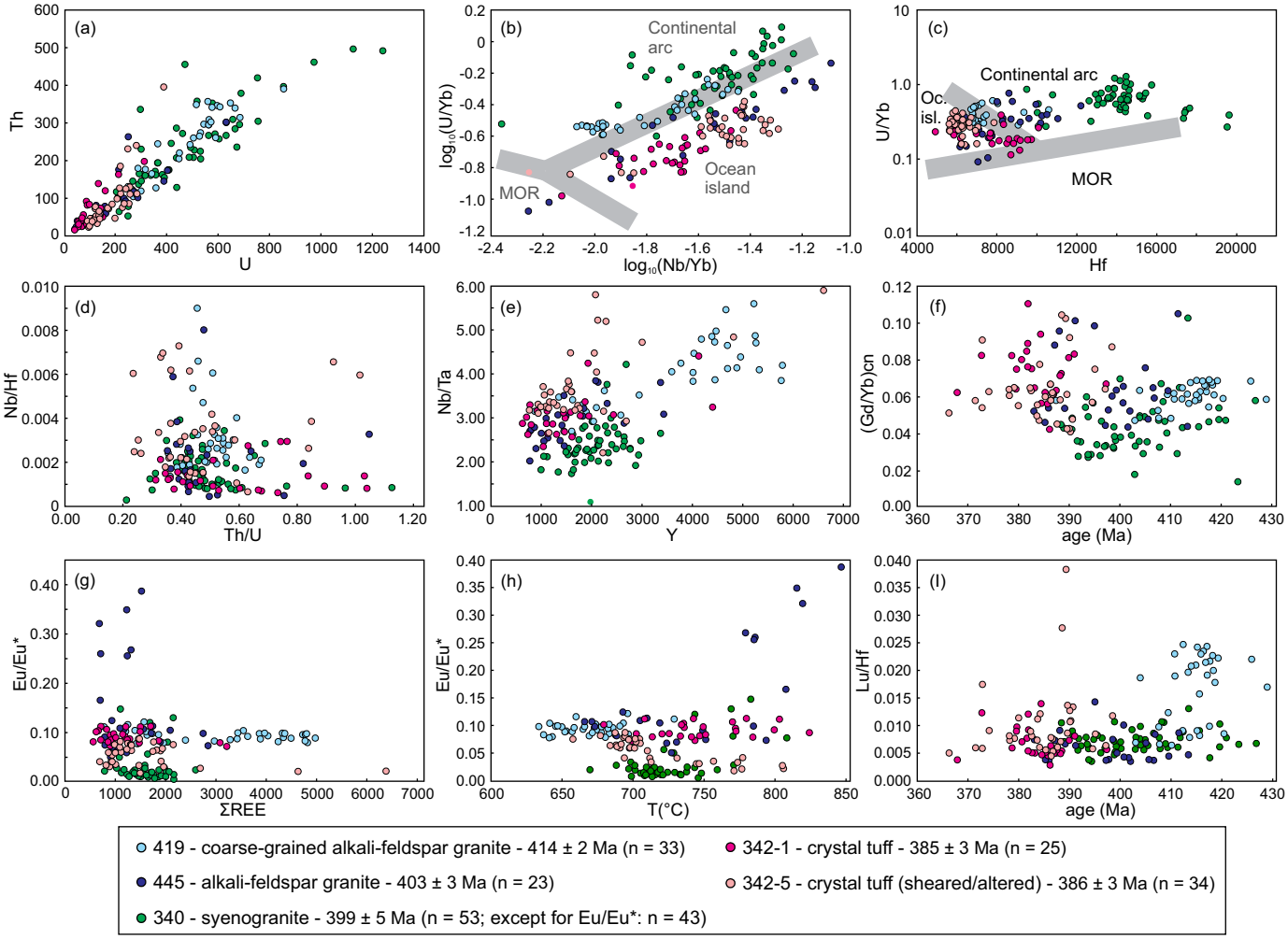

Figure 3. Zircon geochemistry data from Silurian to Devonian grains. Mid-ocean ridge, ocean island and continental arc fields after Grimes *et al.* (2015). Nb/Hf > 0.001 and Nb/Th > 0.05 are characteristic for within-plate/anorogenic/rift settings (Yang *et al.* 2012; cf. Elliott *et al.* 1997). Eu/Eu* values of most zircon is ~0.1 or less, implying a crustal thickness of ~30 km or less (Tang *et al.* 2020). Alkali-feldspar granite sample 445 yielded zircon Eu/Eu* as high as 0.4 suggesting that some zircon crystallized in crust as thick as ~55 km (Tang *et al.* 2020).

signatures or plot along the boundary between the continental arc and oceanic island fields, or in the continental arc field (Figs. 3b, c). The $\varepsilon_{Hf(t)}$ values are between 2.9 and 13.1 and T_{DM} values are 0.52–1.04 Ga (Fig. 5; Supplementary Data Table S7). These values indicate generally derivation of more juvenile crust than the other samples described below.

Sample 445 – alkali-feldspar granite

Zircon grains display euhedral shapes, aspect ratios of 1:1 to 1:4, and concentric and sector zoning (Supplementary Data File S1). Some grains show apparent cores, but they are not truncated by the rims and the cores and rims probably reflect continuous growth. LA-ICP-MS dates of 25 grains are 413 ± 10 Ma to 383 ± 10 Ma (Fig. 2b; Supplementary Data Table S3). A weighted mean date from 18 analyses is 403 ± 3 Ma (MSWD = 1.3, pof = 0.15). It is the same within error as the weighted mean of $^{206}Pb/^{238}U$ dates of 399.7 ± 1.5 Ma (MSWD = 0.11) for twenty analyses reported by Barr *et al.* (2011) and interpreted as the igneous crystallization age. Younger dates are interpreted to be from domains that suffered Pb loss.

Based on geochemistry (Figs. 3g, h), the new data can be divided in groups with high and low Eu/Eu*. These groups are not correlated with age or any particular CL characteristics, but generally the high, 0.25–0.40 Eu/Eu* analyses correspond to those with high temperature estimates based on Ti in zircon (Fig. 3h). U/Yb-Nb/Yb and U/Yb-Hf tectonic discrimination diagrams show predominately ocean island affinity (Figs. 3b, c). The 3.8-6.8 $\varepsilon_{Hf(t)}$ values and T_{DM} of 0.83–0.99 Ga (Fig. 5b; Supplementary Data Table S7) show that this sample is more evolved than the other alkali-feldspar granite (sample 419) described above.

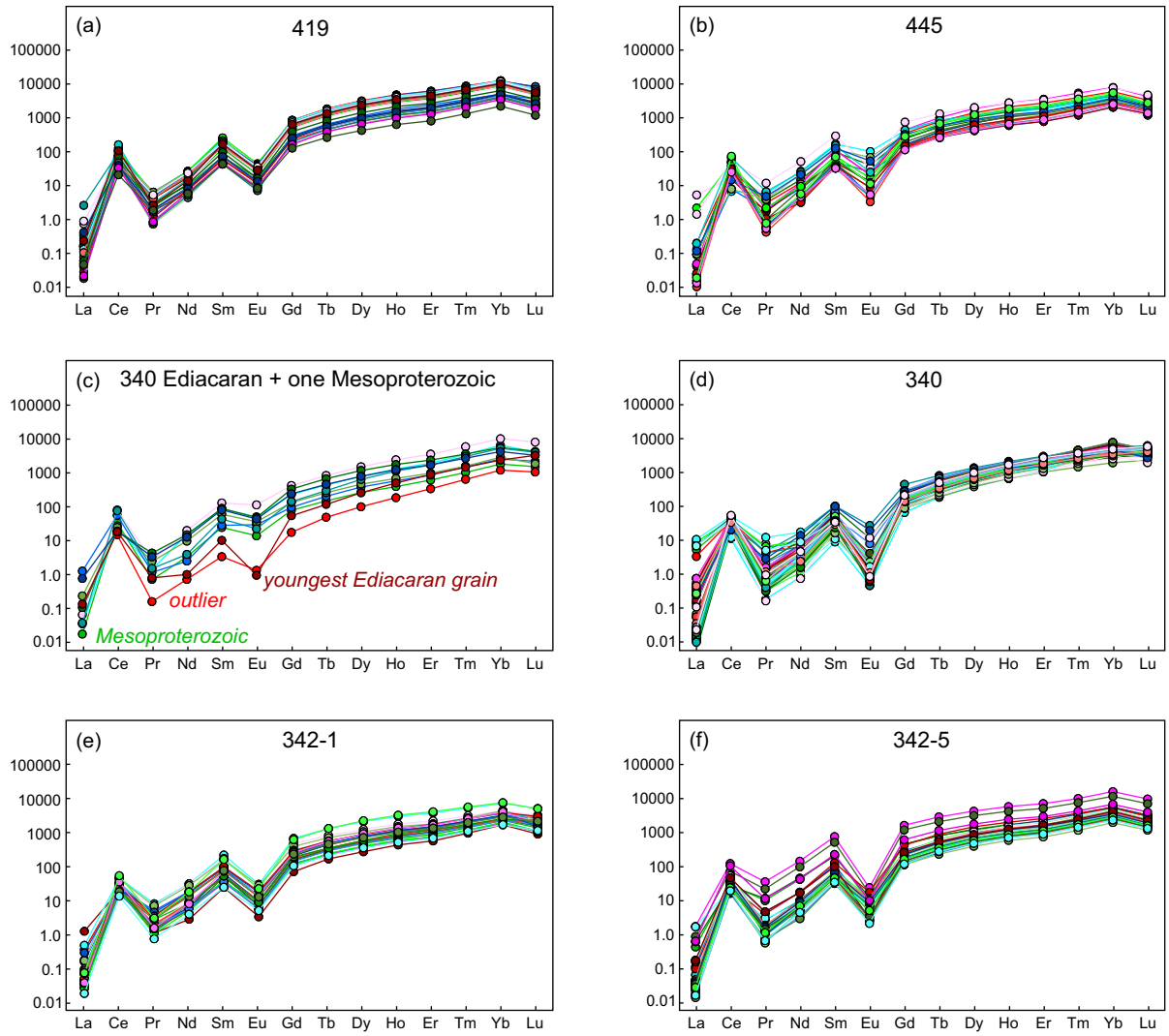

Figure 4. Chondrite-normalized REE patterns of zircon from each sample. CI chondrite normalizing values are from Sun and McDonough (1989). Symbols as in Figure 3.

Sample 340 – syenogranite

Zircon grains are euhedral with aspect ratios of 1:1.5 to 1:3. They typically show concentric zones, and some display cores (Supplementary Data File S1). Sixty-six grains yielded LA-ICP-MS dates of 1281 ± 23 to 388 ± 12 Ma (Figs. 2c–e; Supplementary Data Table S4). A weighted mean date from the 48 youngest dates is 399 ± 5 Ma (MSWD = 1.2, pof = 0.16; Fig. 2e). This date is interpreted as the igneous crystallization age, and somewhat younger than the age of 407.0 ± 1.9 Ma (n = 17, MSWD = 2.3) of Barr *et al.* (2011). Older dates are between 613 ± 15 Ma and 554 ± 29 Ma (9 grains) and 1281 ± 23 Ma (one grain). These dates are interpreted as being from inherited components. Barr *et al.* (2011) also reported one ~614 Ma grain. Younger dates are interpreted as resulting from Pb loss.

Geochemistry of only the youngest group of zircon grains is shown in Figure 3. Neoproterozoic zircon grains have comparable geochemistry but the Eu anomalies are smaller than for the younger zircon (Figs. 4c, d). Zircon grains of the youngest group display lower Eu/Eu*, Nb/Ta, and $(Gd/Yb)_{cn}$ and higher Th, U, and Hf than the other samples (Fig. 3), where $Eu/Eu^* = Eu_{cn}/(Sm_{cn}*Gd_{cn})^{0.5}$ (McLennan 1989) and cn is chondrite normalized. The U/Yb-Nb/Yb and U/Yb-Hf tectonic discrimination diagrams suggest a continental arc setting (Figs. 3b, h). This result is consistent with the calc-alkaline whole-rock $(Na_2O+K_2O)/Al_2O_3$ signature reported by Barr *et al.* (2011).

Zircon $\varepsilon_{Hf(t)}$ values are 3.3–6.8 for the 398 ± 2 Ma grains, 1.6–6.1 for the Ediacaran grains, and 10.0 for the Mesoproterozoic grain (Fig. 5; Supplementary Data Table S7). T_{DM} are 0.84–1.02 Ga for the ~444–384 Ma grains, 1.00–1.26 Ga for the Ediacaran grains, and 1.39 for the Mesoproterozoic grain (Table 1; Supplementary Data Table S7). The youngest zircon population, reflecting crystallization of the syenogranite, has similar age and Hf values as sample 445 (Fig. 5).

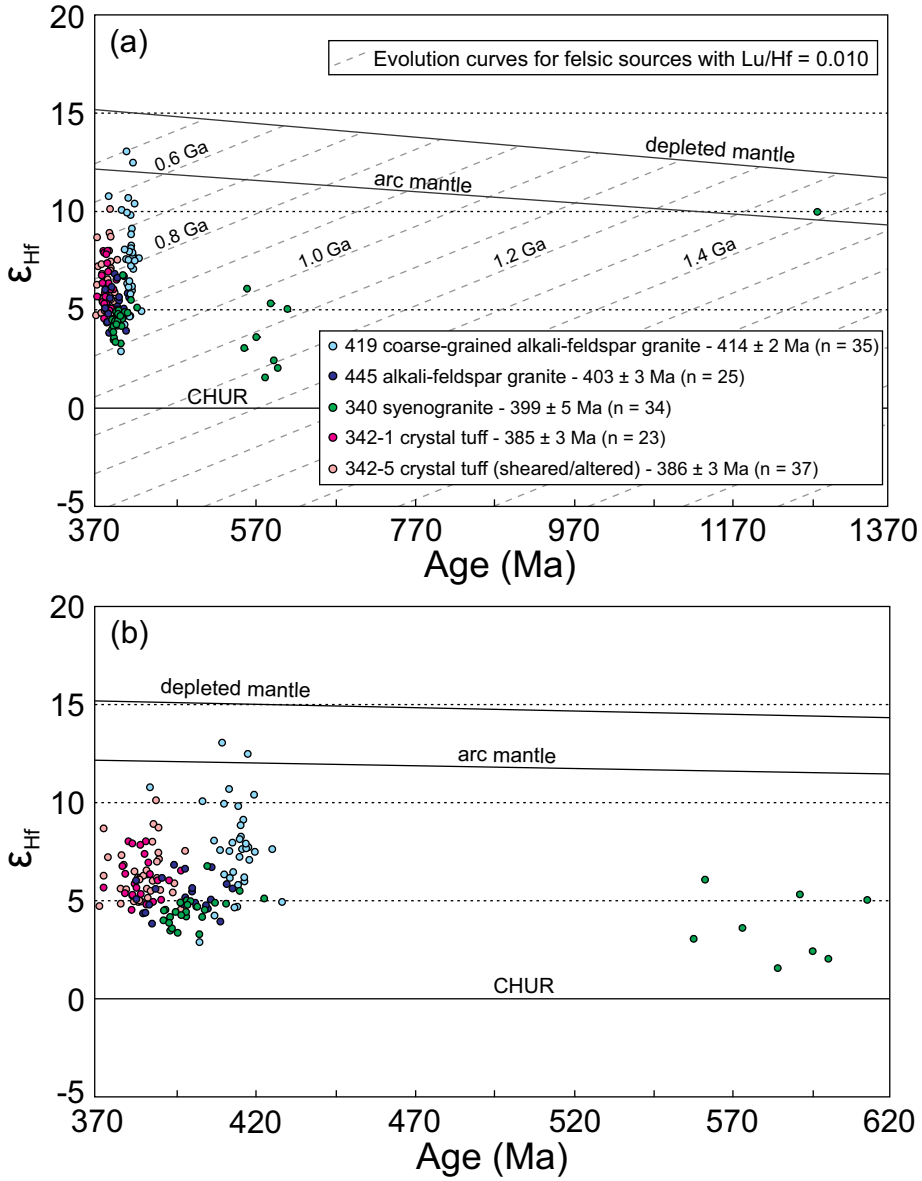

Figure 5. Zircon ε_{Hf} versus age plots.

Sample 342-1 – crystal tuff

Zircon grains are euhedral with generally concentric zoning. Some grains do not show zoning and some show sector and/or patchy zoning (Supplementary Data File S1). Aspect ratios are up to 1:4, whereas some grains are stubby and may represent fragments. Twenty-six grains yielded dates between 397 ± 10 and 368 ± 9 Ma (Fig. 2f; Supplementary Data Table S5). A weighted mean date from 24 dates is 385 ± 3 Ma (MSWD = 1.0, pof = 0.44). This interpreted igneous crystal-lization age is almost identical to the age of 384.4 ± 2.3 Ma determined by Barr *et al.* (2011). Younger dates probably re-sulted from Pb loss. Zircon grains are low in Th and U (Fig. 3a). U/Yb-Nb/Yb and U/Yb-Hf tectonic discrimination diagrams indicate ocean island signatures (Figs. 3b, h). Zircon $\varepsilon_{Hf(t)}$ values are between 4.5 and 8.0 and T_{DM} is 0.75–0.94 Ga (Fig. 5; Supplementary Data Table S7).

Sample 342-5 – crystal tuff (sheared/altered)

Euhedral zircon grains with aspect ratios of 1:1 to 1:4 show generally concentric zones (Supplementary Data File S1). Thirty-eight grains from 342-5 yield LA-ICP-MS dates of 398 ± 10 to 366 ± 7 Ma (Fig. 2g; Supplementary Data Table S6). A weighted mean date from the 33 oldest dates is 386 ± 3 Ma (Fig. 2h; MSWD = 1.4, pof = 0.06). This date is similar within error to the age of 383.9 ± 1.6 Ma reported by Barr *et al.* (2011) and is interpreted as the igneous crystallization age. Younger dates are interpreted to be from domains that suffered Pb loss. The age is also within error of the age of sample 342-1 from the same location. However, sample 342-5 shows higher Eu/Eu*and $(Gd/Yb)_{cn}$ and lower U, Th, Lu/Hf, Nb/Hf, Nb/Ta, and REE than sample 342-1 (Figs. 3, 4e). The U/Yb-Nb/Yb and U/Yb-Hf tectonic discrimination diagrams suggest an ocean island tectonic

setting for both these samples (Figs. 3b, c). The 4.6–10.1 $\varepsilon_{Hf(t)}$ values, 0.65–0.95 Ga T_{DM} (Fig. 5; Supplementary data table S7), and age and zircon chemistry are consistent with the data from sample 342-1.

IMPLICATIONS

Barr *et al.* (2011) and Thompson *et al.* (2018) interpreted the samples from the Gulf of Maine as part of a ~30– >80 km wide zone of mid-Paleozoic alkalic igneous rocks that exists primarily in Avalonia. Sample 419, as well as the samples from sites 421, 423, and 427 (Fig. 1), are located northwest of the Fundy magnetic anomaly zone and hence could have been emplaced in Ganderian crust. No age data are available for samples from sites 421, 423, and 427 in this study or that of Barr *et al.* (2011), but whole-rock chemical data reported by Barr *et al.* (2011) for a tonalitic sample from site 427 do not appear significantly different from those of the granitic samples. Also, photomicrographs published in Hermes *et al.* (1978) show that samples from sites 421 and 423 are similar to the sample from site 419, and all three sites are on the same NE-trending structure (Three Dory Ridge). Hence it seems likely that all the rocks included in the Cashes Ledge igneous suite are of similar age and origin.

Zircon Nb/Hf ratios are generally greater than 0.001 (Fig. 3d), characteristic for within-plate/anorogenic/rift settings, although some are lower and imply an arc/orogenic setting (Yang *et al.* 2012; cf. Elliott *et al.* 1997). Zircon U/Yb-Nb/Yb and U/Yb-Hf tectonic discrimination diagrams (Figs. 3b, c) suggest ocean island to continental arc setting, with the strongest arc signature for ~399 Ma syenogranite sample 340. Europium anomalies ($Eu/Eu^{\star}$) of most zircon grains are ~0.1 or less, implying a crustal thickness of ~30 km or less (Tang *et al.* 2020), consistent with an extensional setting. An extensional setting is consistent with interpretations by Hermes *et al.* (1978), Barr *et al.* (2011) and Thompson *et al.* (2018) based on whole-rock chemical data. Alkali-feldspar granite sample 445 yielded zircon $Eu/Eu^{\star}$ between 0.25 and 0.40 for six zircon grains, suggesting that some zircon crystallized in ~40–55 km thick crust, perhaps reflecting localized Acadian orogenic thickening in Avalonia.

Chondrite-normalized REE patterns of zircon (Fig. 4) show low La, Ce at 100, low Eu and Yb and Lu at 1000–10 000, which are similar to signatures of syenite pegmatite or larvikite of Belousova *et al.* (2002), suggesting fractional crystallization of mafic magmas. Eight Ediacaran and one Mesoproterozoic zircon in sample 340 (Fig. 4c) show higher Eu, but otherwise trends similar to those of the Silurian–Devonian grains.

The four samples southeast of the Fundy anomaly display higher $\varepsilon_{Hf(t)}$ values with decreasing U–Pb age, suggesting increasing input from juvenile material with time, consistent with an extensional setting. The fact that the Silurian-Devonian grains in sample 340 have higher $\varepsilon_{Hf(t)}$ values than the Ediacaran grains in the same sample implies that the syenogranite crystallized from more primitive melt and was not entirely sourced from the Ediacaran arc. This result may also indicate extension. Sample 419 northwest of the Fundy anomaly has the highest $\varepsilon_{Hf(t)}$ values, indicating the most juvenile source of all samples. However, none of the data plot on the depleted mantle curve, suggesting some crustal input in all samples. Zircon Lu–Hf model ages based on felsic sources are 0.52–1.04 Ga, suggesting a mix of late Mesoproterozoic crustal and juvenile sources. Such results are consistent with both Avalonian and Ganderian basement (cf. Pollock *et al.* 2022). Therefore, the question of whether our samples were emplaced in Avalonian or Ganderian crust, and where the terrane boundary is located in the offshore, remains unresolved.

In summary, zircon REE geochemistry and Lu/Hf isotopic data show a generally juvenile source for the zircon of the ~414-385 Ma Cashes Ledge igneous suite. However, for unknown reasons, zircon U/Yb-Nb/Yb and U/Yb-Hf tectonic discrimination diagrams for syenogranite sample 340 show an arc affinity, and $Eu/Eu^{\star}$ ratios for six zircon grains in alkali-feldspar granite sample 445 suggest thickened crust.

CONCLUSIONS

New LA-ICP-MS U–Pb dating and Lu–Hf isotopic analyses of zircon grains from the Cashes Ledge igneous suite in the Gulf of Maine, USA, corroborate earlier petrologi-cal studies and dating results from Barr *et al.* (2011). Three granitic samples are between 414 Ma and 399 Ma, and that two felsic tuff sample are somewhat younger at ~385 Ma. The parent magmas are relatively juvenile with whole-rock ε_{Ndt} -0.5 to 3.7 (Barr *et al.* 2011) and $\varepsilon_{Hf(t)}$ in zircon between 2.9 and 13.1 (this study). They likely formed in a protracted Silurian–Devonian within-plate extensional setting that extends into the onshore in Avalonia in southeastern New England, but may straddle the Avalonia-Ganderia boundary in the Gulf of Maine.

ACKNOWLEDGEMENTS

This manuscript benefited from discussion with Gianna Greger and Margaret Thompson at the 2022 Geological Society of America Northeastern Section meeting, and with Chris White, who initially suggested working on the Gulf of Maine samples collected by Ballard (1974). We are grateful for constructive comments by journal reviewers Sarah Mazza and Mike Dorais, and USGS reviewer Chris Hepburn. Analytical work was supported by NSF grant EAR-1827429. Sandra Barr's research is funded mainly by discovery grants from the Natural Sciences and Engineering Council of Canada. This contribution is part of International Geoscience Programme project IGCP683.

REFERENCES

Allen, C.M. and Campbell, I.H. 2012. Identification and elimination of a matrix-induced systematic error in LA–ICP–MS $^{206}Pb/^{238}U$ dating of zircon. Chemical Geology 332–333, pp. 157–165. https://doi.org/10.1016/j.chemgeo.2012.09.038

Andersen, T., Andersson, U.B., Graham, S., Aberg, G., and Simonsen, S.L. 2009. Granitic magmatism by melting of juvenile continental crust: New constraints on the source of Palaeoproterozoic granitoids in Fennoscandia from Hf isotopes in zircon. Journal of the Geological Society, 166, pp. 233–247. https://doi.org/10.1144/0016-76492007-166

Ballard, R.D. 1974. Summary of the geologic dives conducted in the Gulf of Maine during 1971 and 1972 by the research submersible Alvin. Woods Hole Oceanographic Institution, Technical report WHOI-74-29, unpublished manuscript.

Barr, S.M., Mortensen, J.K., Thompson, M.D., Hermes, O.D., and White, C.E. 2011. Early to Middle Devonian granitic and volcanic rocks from the central Gulf of Maine. Lithos, 126, pp. 455–465. https://doi.org/10.1016/j.lithos.2011.06.009

Belousova, E., Griffin, W., O'Reilly, S.Y., and Fisher, N. 2002. Igneous zircon: trace element composition as an indicator of source rock type. Contributions to Mineralogy and Petrology, 143, pp. 602–622. https://doi.org/10.1007/s00410-002-0364-7

Bouvier, A., Vervoort, J.D., and Patchett, P.J. 2008. The Lu–Hf and Sm-Nd isotopic composition of CHUR: Constraints from unequilibrated chondrites and implications for the bulk composition of terrestrial planets. Earth and Planetary Science Letters, 273, pp. 48–57. https://doi.org/10.1016/j.epsl.2008.06.010

Chu, N.C., Taylor, R.N., Chavagnac, V., Nesbitt, R.W., Boella, R.M., Milton, J.A., German, C.R., Bayon, G., and Burton, K. 2002. Hf isotope ratio analysis using multi-collector inductively coupled plasma mass spectrometry: an evaluation of isobaric interference corrections. Journal of Analytica Atomic Spectrometry, 17, pp. 1566-1674. https://doi.org/10.1039/b206707b

Dhuime, B., Hawkesworth, C., and Cawood, P. 2011. When continents formed. Science, 331, 154–155. https://www.science.org/doi/10.1126/science.1201245

Elliott, T., Plank, T., Zindler, A., White, W., and Bourdon, B. 1997. Element transport from slab to volcanic front at the Mariana arc. Journal of Geophysical Research, 102, pp. 14991–15019. https://doi.org/10.1029/97JB00788

Griffin, W.L., Pearson, N.J., Belousova, E., Jackson, S.E., van Achterbergh, E., O'Reilly, S.Y., and Shee, S.R. 2000. The Hf isotope composition of cratonic mantle: LAM-MC-ICPMS analysis of zircon megacrysts in kimberlites. Geochimica et Cosmochimica Acta, 64, pp. 133–147. https://doi.org/10.1016/S0016-7037(99)00343-9

Grimes, C.B., Wooden, J.L., Cheadle, M.J., and John, B.E. 2015. "Fingerprinting" tectono-magmatic provenance using trace elements in igneous zircon. Contributions to Mineralogy and Petrology, 170, pp. 1–26. https://doi.org/10.1007/s00410-015-1199-3

Hermes, O.D., Ballard, R.D., and Banks, P.O. 1978. Upper Ordovician peralkalic granites from the Gulf of Maine. Geological Society of America Bulletin, 89, pp. 1761–1774. https://doi.org/10.1130/0016-7606(1978)89<1761:UOPGFT>2.0.CO;2

Hibbard, J.P., van Staal, C.R., Rankin, D., and Williams H. 2006. Lithotectonic map of the Appalachian orogen (north), Canada-United States of America. Geological Survey of Canada Map 02041A, 1 sheet, scale 1:1 500 000. https://doi.org/10.4095/221912

Hutchinson, D.R., Klitgord, K.D., Lee, M.W., and Trehu, A.M. 1988. U.S. Geological Survey deep seismic profile across the Gulf of Maine. Geological Society of America Bulletin, 100, 172–184. https://doi.org/10.1130/0016-7606(1988)100<0172:USGSDS>2.3.CO;2

Kay, A., Hepburn, J.C., Kuiper, Y.D., and Baxter, E.F. 2017. Geochemical evidence for a Ganderian arc/back-arc remnant in the Nashoba terrane, SE New England, USA. American Journal of Science, 317, pp. 413–448. https://doi.org/10.2475/04.2017.01

Kuiper, Y.D., Murray, D.P., Ellison, S., and Crowley, J.L. 2022. U–Pb detrital zircon analysis of sedimentary rocks of the southeastern New England Avalon terrane in the U.S. Appalachians: Evidence for a separate crustal block. *In* New Developments in the Appalachian-Caledonian-Variscan Orogen. *Edited by* Y.D. Kuiper, J.B. Murphy, R.D. Nance, R.A. Strachan and M.D. Thompson, Geological Society of America, Special Paper, 554, pp. 93–119. https://doi.org/10.1130/2021.2554(05)

Ludwig, K.R. 2003. User's Manual for Isoplot 3.00. Berkeley Geochronology Center. Berkeley, CA, 70 p. https://searchworks.stanford.edu/view/6739593

McLennan, S.M. 1989. Rare earth elements in sedimentary rocks: Influence of provenance and sedimentary process. *In* Chapter 7, Reviews in Mineralogy, 21, pp. 169–200. https://doi.org/10.1515/9781501509032-010

Murphy, J.B. and Nance, R.D. 2002. Sm–Nd isotopic systematics as tectonic tracers: An example from West Avalonia in the Canadian Appalachians. Earth-Science Reviews, 59, pp. 77–100. https://doi.org/10.1016/S0012-8252(02)00070-3

Murphy, J.B., Nance, R.D., and Wu, L. 2023. The provenance of Avalonia and its tectonic implications: a critical reappraisal. *In* The Consummate Geoscientist: A Celebration of the Career of Maarten de Wit. *Edited by* A.J. Hynes and J.B. Murphy. Geological Society, London, Special Publications 531, pp. 176–197. https://doi.org/10.1144/SP531-2022-176

Nance, R.D., Murphy, B.J., Strachan, R.A., Keppie, J.D., Gutiérrez-Alonso, G., Fernández-Suárez, J., Quesada, C., Linnemann, U., D'lemos, R., and Pisarevsky, P.A. 2008. Neoproterozoic-early Palaeozoic tectonostratigraphy and palaeogeography of the peri-Gondwanan terranes: Amazonian,West African connections. Geological Society of London, Special Publications, 297, pp. 345–383. https://

doi.org/10.1144/SP297.17

Patchett, P.J., Kouvo, O., Hedge, C.E., and Tatsumoto, M. 1982. Evolution of continental crust and mantle heterogeneity: evidence from Hf isotope. Contributions to Mineralogy and Petrology, 78, pp. 279–297. https://doi.org/10.1007/bf00398923

Paton, C., Hellstrom, J., Paul, B., Woodhead, J., and Hergt, J. 2011. Iolite: Freeware for the visualization and processing of mass spectrometric data. Journal of Analytical Atomic Spectrometry, 26, pp. 2508–2518. https://doi.org/10.1039/c1ja10172b

Pietranik, A.B., Hawkesworth, C.J., Storey, C.D., Kemp, A.I.S., Sircombe, K.N., Whitehouse, M.J., and Bleeker, W. 2008. Episodic, mafic crust formation from 4.5 to 2.8 Ga: New evidence from detrital zircons, Slave craton, Canada. Geology, 36, pp. 875–878. https://doi.org/10.1130/G24861A.1

Pollock, J.C., Hibbard, J.P., and van Staal, C.R. 2012. A paleogeographical review of the peri-Gondwanan realm of the Appalachian orogeny. Canadian Journal of Earth Sciences, 49, pp. 259–288. https://doi.org/10.1139/e11-049

Pollock, J.C., Barr, S.M., van Rooyen, D., and White, C.E. 2022. Insights from Lu–Hf zircon isotopic data on the crustal evolution of Avalonia and Ganderia in the northern Appalachian orogen. *In* New Developments in the Appalachian-Caledonian-Variscan Orogen. *Edited by* Y.D. Kuiper, J.B. Murphy, R.D. Nance, R.A. Strachan and M.D. Thompson, Geological Society of America, Special Paper, 554, pp. 173–207. https://doi.org/10.1130/2021.2554(08)

Samson, S.D., Barr, S.M., and White, C.E. 2000. Nd isotopic characteristics of terranes within the Avalon zone, southern New Brunswick. Canadian Journal of Earth Sciences, 37, p. 1039–1052. https://doi.org/10.1139/e00-015

Severson, A.R., Kuiper, Y.D., Eby, G.N., Lee, H.-Y., and Hepburn, J.C. 2022. New detrital zircon U–Pb ages and Lu–Hf isotopic data from metasedimentary rocks along the western boundary of the composite Avalon terrane in the southeastern New England Appalachians. *In* New Developments in the Appalachian-Caledonian-Variscan Orogen. *Edited by* Y.D. Kuiper, J.B. Murphy, R.D. Nance, R.A. Strachan and M.D. Thompson, Geological Society of America, Special Paper, 554, pp. 73–91. https://doi.org/10.1130/2021.2554(04)

Skehan, J.W. and Rast, N. 1990. Pre-Mesozoic evolution of Avalon terranes of southern New England. *In* Geology of the Composite Avalon Terrane of Southern New England. *Edited by* A.D. Socci, J.W. Skehan, and G.W. Smith. Geological Society of America, Special Paper, 245, pp. 13–53. https://doi.org/10.1130/SPE245-p13

Sláma, J., Košler, J, Condon, D.J., Crowley, J.L., Gerdes, A., Hanchar, J.M., Horstwood, M.S.A., Morris, G.A., Nasdala, L., Norberg, N., Schaltegger, U., Schoene, B. Tubrett, M.N., and Whitehouse, M.J. 2008. Plešovice zircon — A new natural reference material for U–Pb and Hf isotopic microanalysis. Chemical Geology, 249, pp. 1–35. https://doi.org/10.1016/j.chemgeo.2007.11.005

Söderlund, U., Isachsen, C.E., Bylund, G., Heaman, L.M., Patchett, P.J., Vervoort, J.D., and Andersson, U.B. 2005. U–Pb baddeleyite ages and Hf, Nd isotope chemistry constraining repeated mafic magmatism in the Fennoscandian Shield from 1.6 to 0.9 Ga. Contributions to Mineralogy and Petrology, 150, pp. 174–194. https://doi.org/10.1007/s00410-005-0011-1

Souders A.K., Sylvester P.J., and Myers J.S. 2013. Mantle and crustal sources of Archean anorthosite: a combined in situ isotopic study of Pb–Pb in plagioclase and Lu–Hf in zircon. Contributions to Mineralogy and Petrology, 165, 1–24. https://doi.org/10.1007/s00410-012-0789-6

Sun S. and McDonough, W.F. 1989. Chemical and isotopic systematics of oceanic basalts: implications for mantle composition and processes. *In* Magmatism in the ocean basins. *Edited by* A.D. Saunders and M J. Norry. Geological Society Special Publications, 42, pp. 313–345. https://doi.org/10.1144/GSL.SP.1989.042.01.19

Swanson-Hysell, N.L., Hoaglund, S.A., Crowley, J.L., Schmitz, M.D., Zhang, Y., and Miller, J.D. 2020. Rapid emplacement of massive Duluth Complex intrusions within the North American Midcontinent Rift. Geology, 49, pp. 185–189. https://doi.org/10.1130/G47873.1

Tang, M., Ji, W.-Q., Chu, X, Wu, A., and Chen, C. 2020. Reconstructing crustal thickness evolution from europium anomalies in detrital zircons. Geology, 49, pp. 76–80. https://doi.org/10.1130/G47745.1

Thompson, M.D., Barr, S.M., and Grunow, A.M. 2012. Avalonian perspectives on Neoproterozoic paleogeography: Evidence from Sm-Nd isotope geochemistry and detrital zircon geochronology in SE New England, USA. Geological Society of America Bulletin, 124, pp. 517–531. https://doi.org/10.1130/B30529.1

Thompson, M.D., Ramezani, J., and Grunow, A.M. 2018. Within-Plate Setting of Paleozoic Alkalic Suites in Southeastern New England, USA: Constraints from Chemical Abrasion–TIMS U–Pb Geochronology and Paleomagnetism. The Journal of Geology, 126, pp. 41–61. https://doi.org/10.1086/694867

Thompson, M.D., Barr, S.M., and Pollock, J.C. 2022. Evolving views of West Avalonia: Perspectives from southeastern New England, USA. *In* New Developments in the Appalachian-Caledonian-Variscan Orogen. *Edited by* Y.D. Kuiper, J.B. Murphy, R.D. Nance, R.A. Strachan and M.D. Thompson, Geological Society of America, Special Paper, 554, pp. 47–72. https://doi.org/10.1130/2022.2554(03)

Van Staal, C.R., Whalen, J.B., Valverde-Vaquero, P., Zagorevski, A., and Rogers, N. 2009. Pre-Carboniferous, episodic accretion-related, orogenesis along the Laurentian margin of the northern Appalachians. *In* Ancient orogens and modern analogues. *Edited by* J.B. Murphy, J.D. Keppie and A.J. Hynes. Geological Society, London, Special Publications, 327, pp. 271–316. https://doi.org/10.1144/SP327.13

Van Staal, C.R., Barr, S.M., McCausland, P.M., Thompson, M.D., and White, C.E. 2021a. Tonian-Ediacaran tectonomagmatic evolution of West Avalonia and its Ediacaran-Early Cambrian interactions with Ganderia: an

example of complex terrane transfer due to arc-arc collision? *In* Pannotia to Pangaea: Neoproterozoic and Paleozoic Orogenic Cycles in the Circum-Atlantic Region. *Edited by* J.B. Murphy, R.A. Strachan, and C. Quesada. Geological Society, London, Special Publications, 503, 143–167. https://doi.org/10.1144/SP503-2020-23

Van Staal, C.R., Barr, S.M., Waldron, J.W.F., Schofield, D.I., Zagorevski, A., and White, C.E. 2021b. Provenance and Paleozoic tectonic evolution of Ganderia and its relationships with Avalonia and Megumia in the Appalachian-Caledonide orogen. Gondwana Research, 98, pp. 212–243. https://doi.org/10.1016/j.gr.2021.05.025

Watson, E.B., Wark, D.A., and Thomas, J.B. 2006. Crystallization thermometers for zircon and rutile. Contributions to Mineralogy and Petrology, 151, pp. 413–433. https://doi.org/10.1007/s00410-006-0068-5

White, C.E., Barr, S.M., Hamilton, M.A., and Murphy, J.B. 2021. Age and tectonic setting of Neoproterozoic granitoid rocks, Antigonish Highlands, Nova Scotia, Canada: Implications for Avalonia in the northern Appalachian orogen. Canadian Journal of Earth Sciences, 58, pp. 396–412. https://doi.org/10.1139/cjes-2020-0110

Wiedenbeck, M., Alle, P., Corfu, F., Griffin, W. , Meier, M., Oberli, F., Quadt, A.V., Roddick, J., and Spiegel, W. 1995. Three natural zircon standards for U–Th–Pb, Lu–Hf, trace element and REE Analyses. Geostandards Newsletter, 19, pp. 1–23. https://doi.org/10.1111/j.1751-908X.1995.tb00147.x

Yang, J., Cawood, P.A., Du, Y., Huang, H., Huang, H., and Tao, P. 2012. Large Igneous Province and magmatic arc sourced Permian–Triassic volcanogenic sediments in China. Sedimentary Geology, 261–262, pp. 120–131. https://doi.org/10.1016/j.sedgeo.2012.03.018

Editorial responsibility: *David P. West, Jr.*

APPENDIX

Zircon was analyzed for U–Pb isotopes and zircon trace element geochemistry by laser ablation inductively coupled plasma mass spectrometry (LA-ICP-MS) using two different platforms. Five samples were analyzed with a Thermo-Electron X-Series II quadrupole ICP-MS and New Wave Research UP-213 Nd:YAG UV (213 nm) laser ablation system. One of these samples was also analysed using an iCAP RQ Quadrupole ICP-MS and Teledyne Photon Machines Analyte Excite+ 193 nm excimer laser ablation system with HelEx II Active two-volume ablation cell. Details of the instrumentation are in Supplementary Data tables S2–6. In-house analytical protocols, standard materials, and data reduction software were used for acquisition and calibration of U–Pb dates and a suite of high field strength elements (HFSE) and rare earth elements (REE). Background count rates for each analyte were obtained prior to each spot analysis and subtracted from the raw count rate for each analyte. Ablation pits that appear to have intersected glass or mineral inclusions were identified based on Ti and P. U–Pb dates from these analyses are considered valid if the U/Pb ratios appear to have been unaffected by the inclusions. Analyses that appear contaminated by common Pb were rejected based on mass 204 being above baseline. For concentration calculations, background-subtracted count rates for each analyte were internally normalized to ^{29}Si and calibrated with respect to NIST SRM-610 and -612 glasses as the primary standards. Temperature was calculated from the Ti-in-zircon thermometer (Watson *et al.* 2006). Because there are no constraints on the activity of TiO_2, an average value in crustal rocks of 0.8 was used.

For U–Pb and ^{207}Pb/^{206}Pb dates, instrumental fractionation of the background-subtracted ratios was corrected and dates were calibrated with respect to interspersed measurements of zircon standards and reference materials. The primary standard Plešovice zircon (Sláma *et al.* 2008) was used to monitor time-dependent instrumental fractionation based on two analyses for every 10 analyses of unknown zircon. A secondary correction to the ^{206}Pb/^{238}U dates was made based on results from the zircon standards Seiland (531 Ma, Kuiper *et al.* 2022), FC1 (1095 Ma, Swanson-Hysell *et al.* 2020), and 91500 (Wiedenbeck *et al.* 1995), which were treated as unknowns and measured once for every 10 analyses of unknown zircon. These results showed a linear age bias of several percent that is related to the ^{206}Pb count rate. The secondary correction is thought to mitigate matrix-dependent variations due to contrasting compositions and ablation characteristics between the Plešovice zircon and other standards (and unknowns).

Radiogenic isotope ratio and age error propagation for all analyses includes uncertainty contributions from counting statistics and background subtraction. For groups of analyses that are collectively interpreted from a weighted mean date (i.e., igneous zircon analyses), a weighted mean date is first calculated from equivalent dates (probability of fit >0.05) using Isoplot 3.0 (Ludwig 2003) with errors on individual dates that do not include a standard calibration uncertainty. A standard calibration uncertainty is then propagated into the error on the date. This uncertainty is the local standard deviation of the polynomial fit to the interspersed primary standard measurements versus time for the time-dependent, relatively larger U/Pb fractionation factor, and the standard error of the mean of the consistently time-invariant and smaller ^{207}Pb/^{206}Pb fractionation factor. Standard calibration uncertainties are given in Supplementary Data tables S2–6. Errors without and with the standard calibration uncertainty are shown in the data tables. Errors on single analyses without the standard calibration uncertainty are used in the text. Age interpretations are based on ^{206}Pb/^{238}U dates. Errors are at 2σ.

Hf isotopic compositions of zircon grains (Supplementary Data Table S7) were determined by LA-MC-ICP-MS using a Nu Plasma II MC-ICP-MS coupled to a Australian Scientific Instruments/Applied Spectra RESOlution-SE 193 nm exciter laser system in the USGS PlasmaLab. A 38 μm laser spot was focused on each zircon grain directly on top

of the U–Pb analysis location, firing at a frequency of 10 Hz with an energy density of 7 J/cm^2 for 400 laser pulses. ^{171}Yb, ^{172}Yb, ^{173}Yb, ^{174}(Hf + Yb), ^{175}Lu, ^{176}(Hf + Yb + Lu), ^{177}Lu, ^{178}Hf, ^{179}Hf, and ^{180}Hf were simultaneously measured in 10 Faraday collectors. Each analysis consists of 15 seconds of gas background measurement, followed by 40 seconds of laser ablation, and ending with 15 seconds of monitored wash out. Isotope measurements were acquired using a 0.2 second on-peak integration time. Raw data are processed off-line in Iolite (Paton *et al.* 2011) using the Hf Isotopes data reduction scheme (DRS).

Mass bias factors (β) for Yb and Hf were calculated using the exponential lase and the invariant ^{173}Yb/^{171}Yb ratio of 1.132685 (Chu *et al.* 2002) and the ^{179}Hf/^{177}Hf ratio of 0.732500 (Patchett *et al.* 1982), respectively. The β(Yb) is used as an approximation for β(Lu) since the two isotopes are chemically similar and only two Lu isotopes are found in nature. To determine the ^{176}Hf signal intensity, the ^{176}Yb and ^{176}Lu interferences on the 176-mass must be removed. Interference-free ^{173}Yb and ^{175}Lu were measured and the ^{176}Yb and ^{176}Lu contributions to the measured 176-mass were calculated using the ^{176}Yb/^{173}Yb ratio of 0.796218 (Chu *et al.* 2002) and the ^{176}Lu/^{175}Lu ratio of 0.02656 (Chu *et al.* 2002). The ^{176}Hf/^{177}Hf, ^{176}Yb/^{177}Hf, ^{176}Lu/^{177}Hf, and ^{178}Hf/^{177}Hf are calculated and corrected for instrumental mass bias using β(Hf).

For unknown zircon grains, the initial ^{176}Hf/^{177}Hf ratios were calculated using the measured ^{176}Lu/^{177}Hf ratio for each zircon. The ^{176}Lu decay constant used is 1.867×10^{-11}/yr (Söderlund *et al.* 2004). Also used were chondritic values of ^{176}Hf/^{177}Hf = 0.0336 and ^{176}Lu/^{177}Hf = 0.282785 (Bouvier *et al.* 2008), a model depleted mantle with present day ^{176}Hf/^{177}Hf ratio of 0.28325 and ^{176}Lu/^{177}Hf ratio of 0.0388 (Griffin *et al.* 2000; updated by Andersen *et al.* 2009), ^{176}Lu/^{177}Hf ratios of mafic and felsic crust of 0.022 and 0.010, respectively (Pietranik *et al.* 2008), and a model arc mantle with present day ε_{Hf} of 13.2, ^{176}Hf/^{177}Hf = 0.283158 and ^{176}Lu/Hf = 0.03786 (Dhuime *et al.* 2011, using CHUR values of Bouvier et al. 2008).

URL links to Supplementary Data

Supplementary Data File S1: https://journals.lib.unb.ca/index.php/ag/article/view/33388/1882529035
Supplementary Date Table S2: https://journals.lib.unb.ca/index.php/ag/article/view/33388/1882529036
Supplementary Date Table S3: https://journals.lib.unb.ca/index.php/ag/article/view/33388/1882529037
Supplementary Date Table S4: https://journals.lib.unb.ca/index.php/ag/article/view/33388/1882529038
Supplementary Date Table S5: https://journals.lib.unb.ca/index.php/ag/article/view/33388/1882529039
Supplementary Date Table S6: https://journals.lib.unb.ca/index.php/ag/article/view/33388/1882529040
Supplementary Date Table S7: https://journals.lib.unb.ca/index.php/ag/article/view/33388/1882529041

Supplementary Data File S1

419-1-2 Large

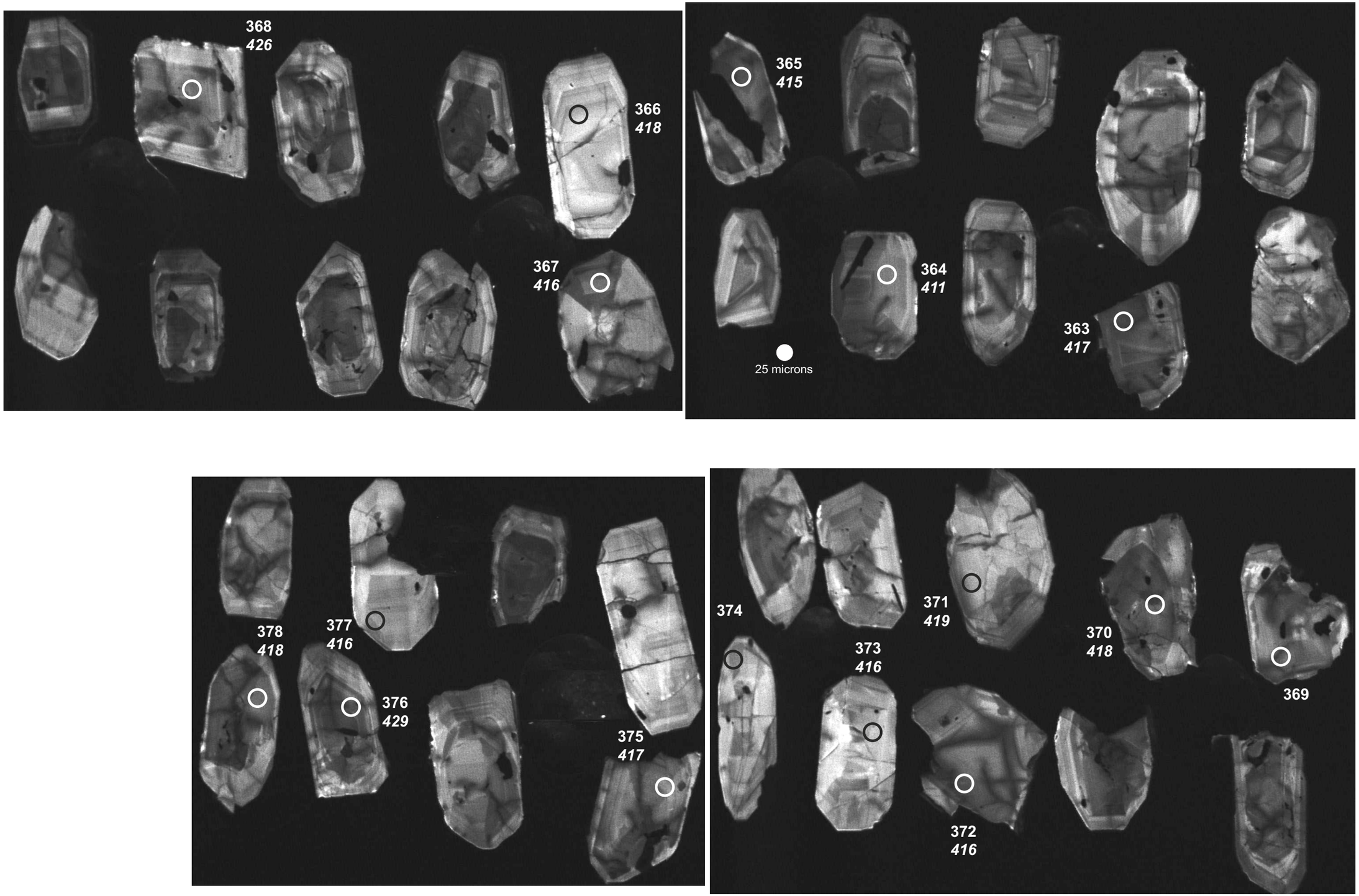

419-1-2 Medium

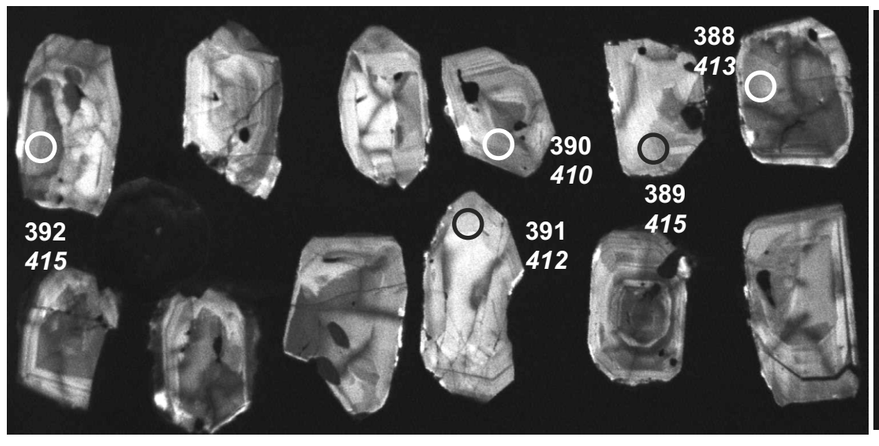

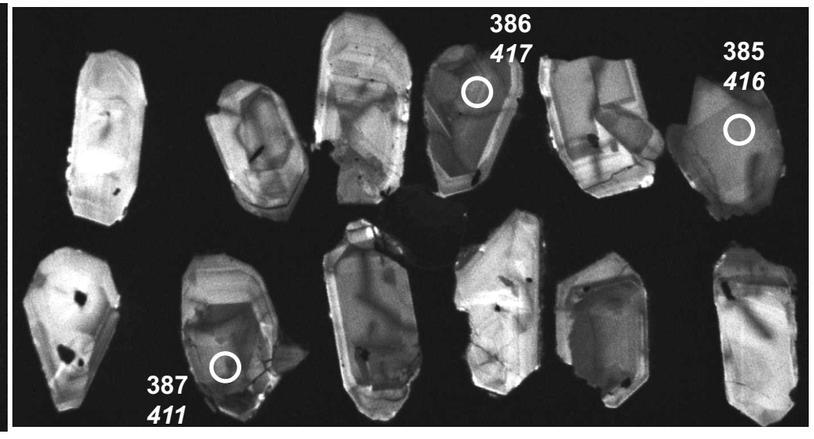

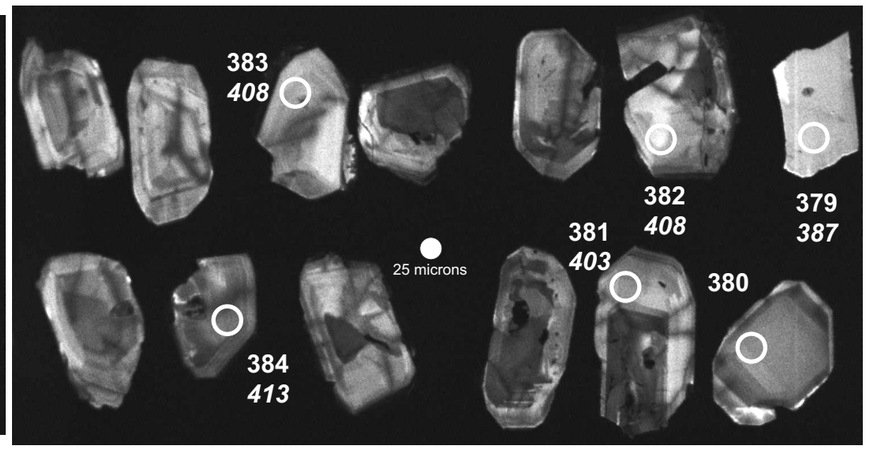

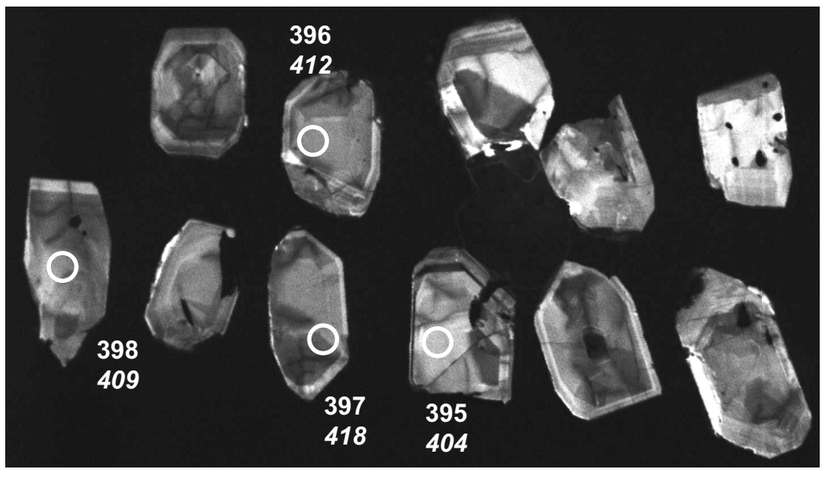

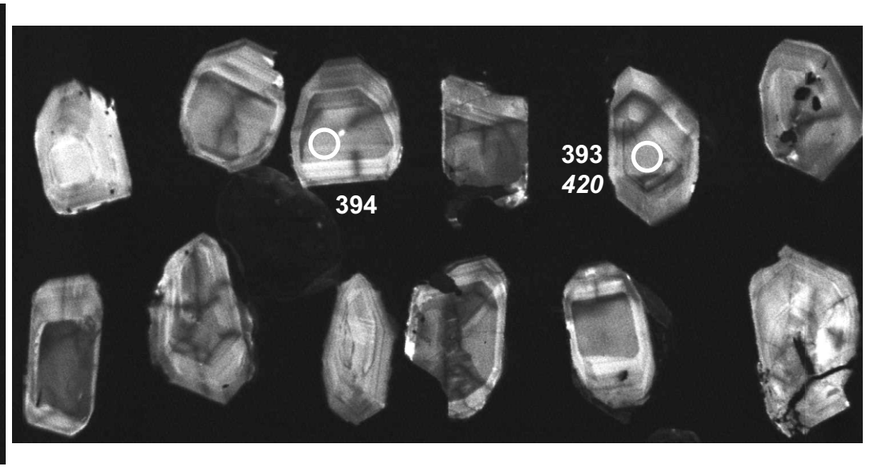

419-1-2 Small

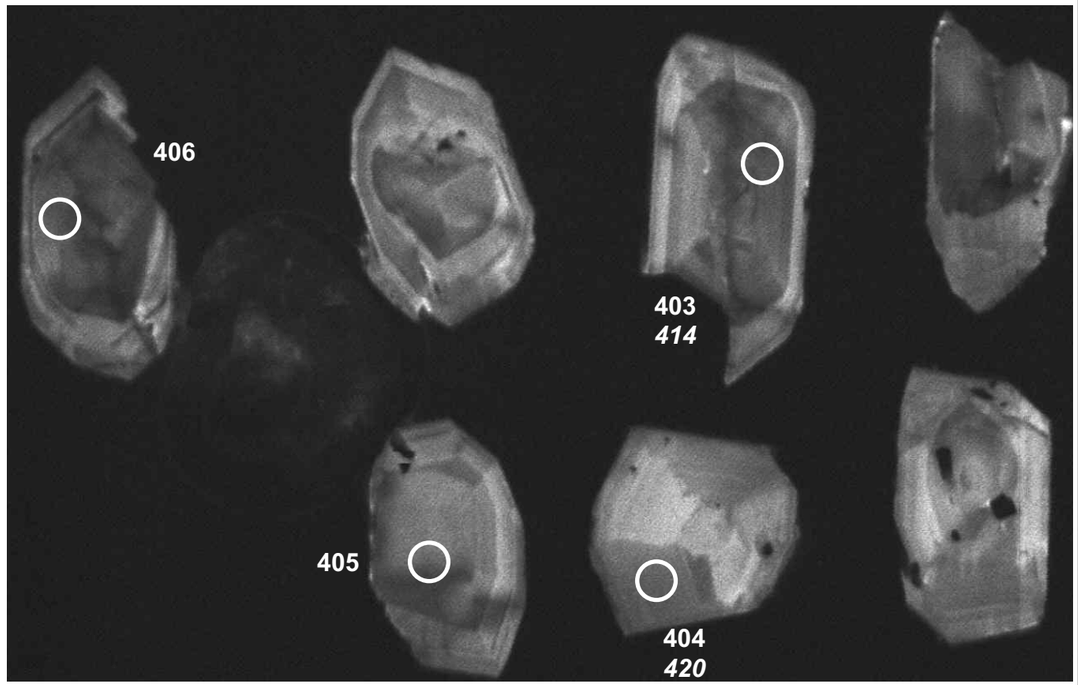

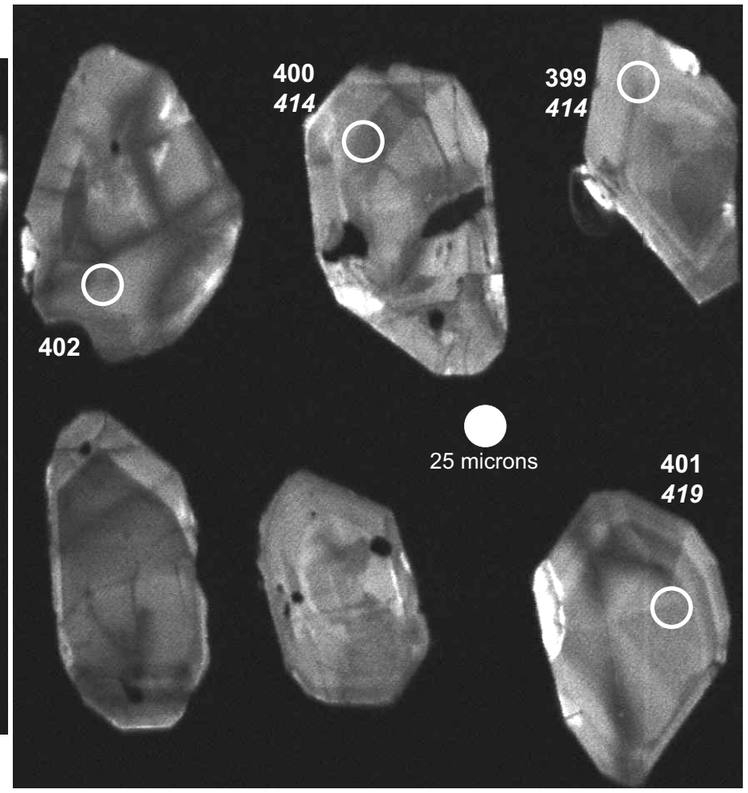

445-2-2 Large

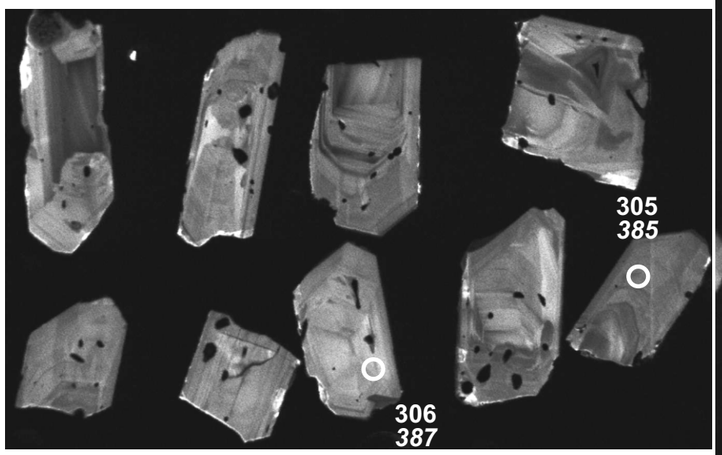
305
385
306
387

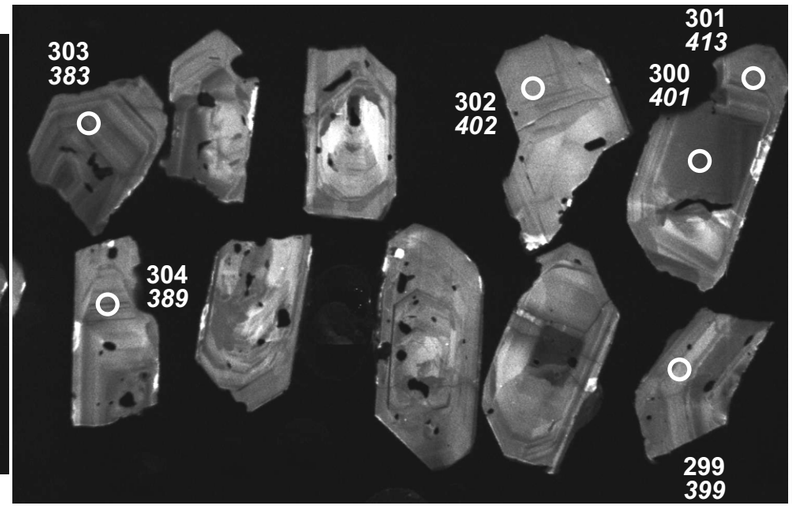
303
383
304
389
302
402
301
413
300
401
299
399

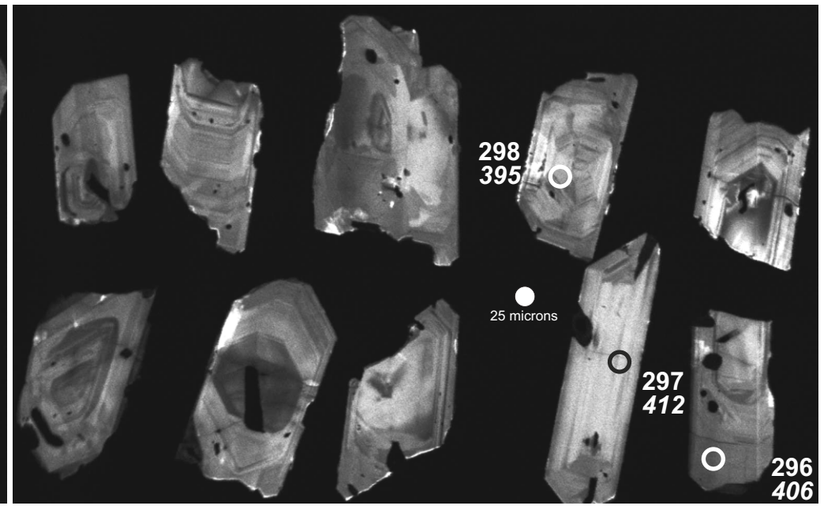
298
395
25 microns
297
412
296
406

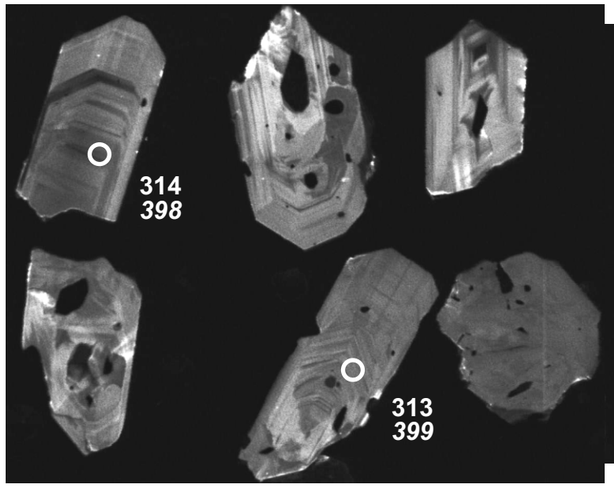
314
398
313
399

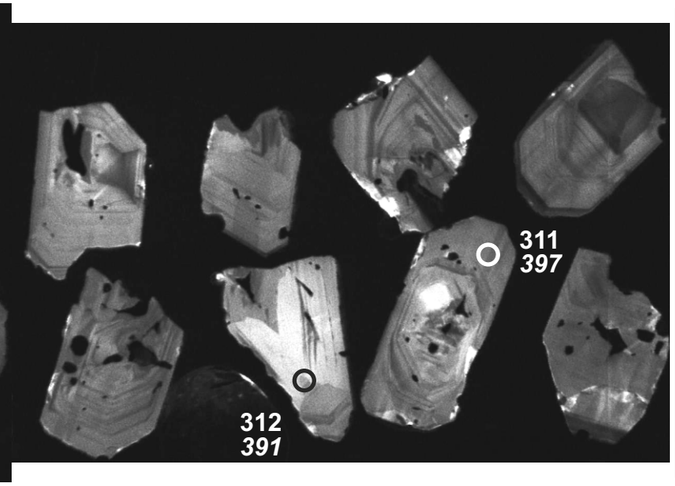
311
397
312
391

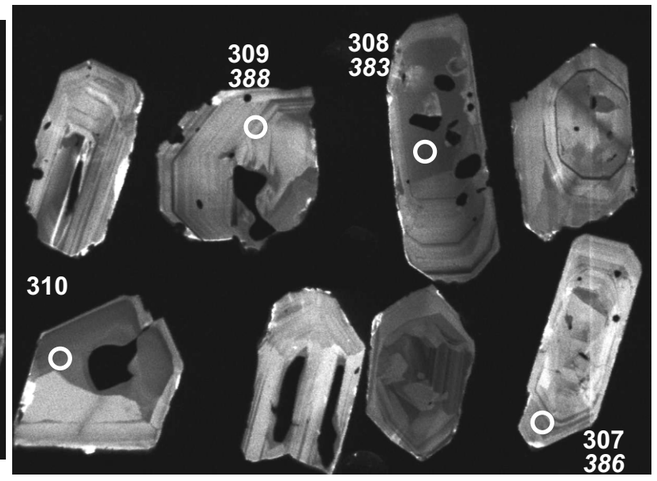
309
388
308
383
310
307
386

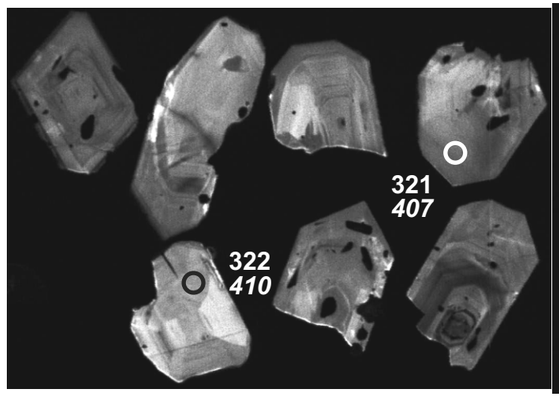
321
407
322
410

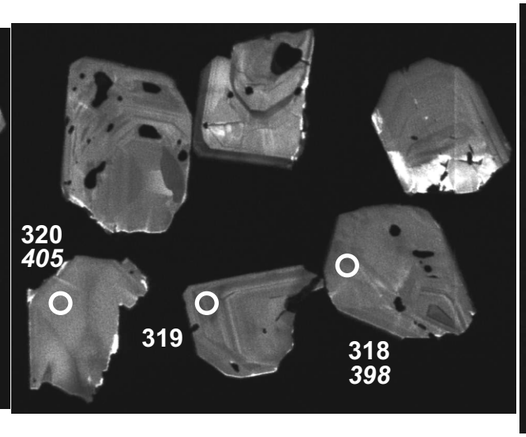
320
405
319
318
398

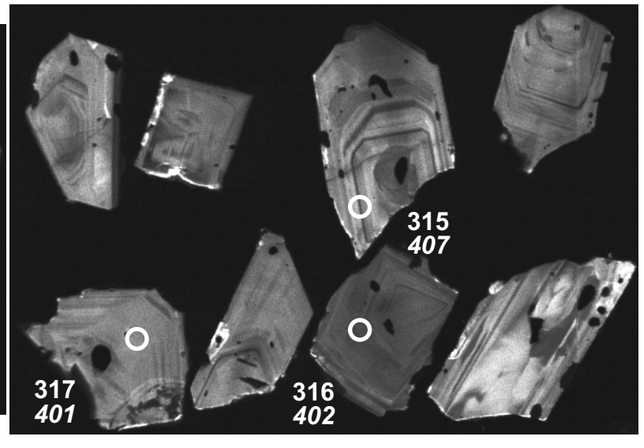
315
407
317
401
316
402

445-2-2 Medium

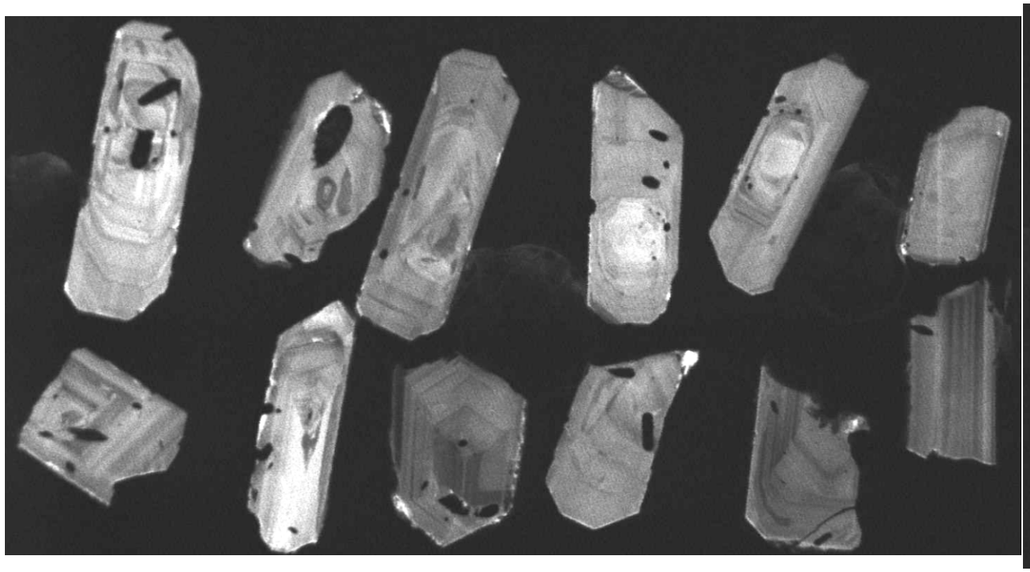

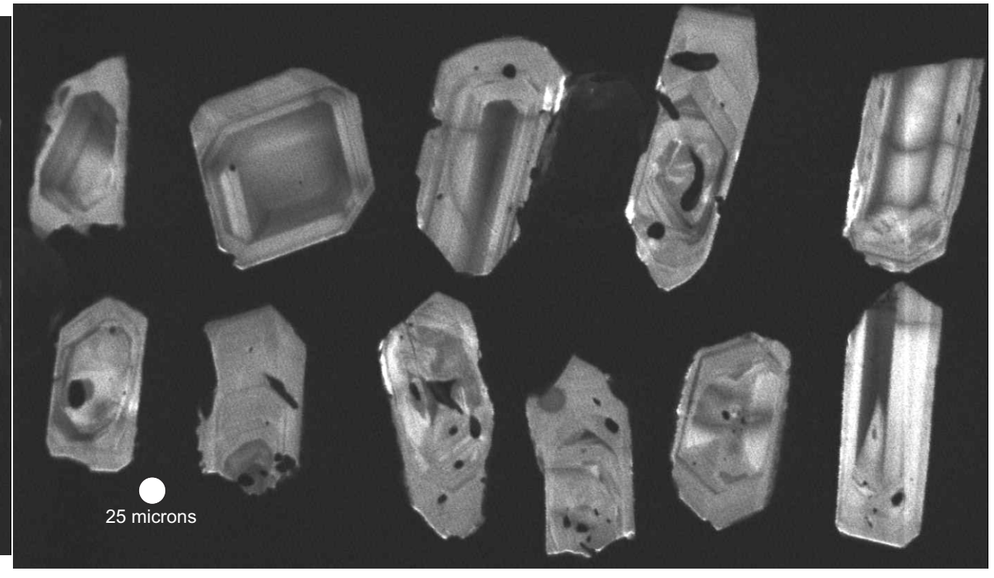

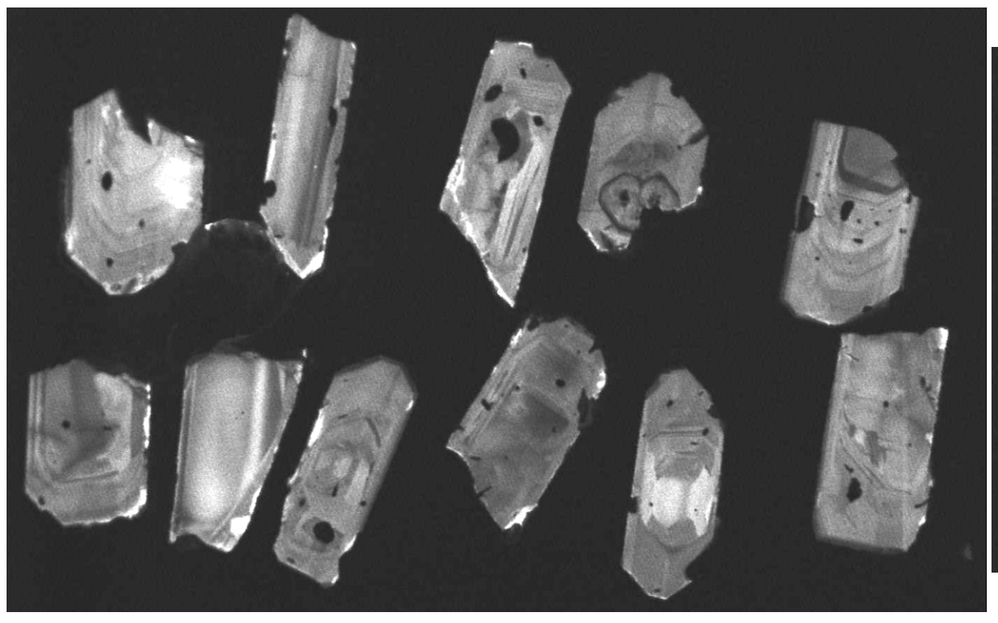

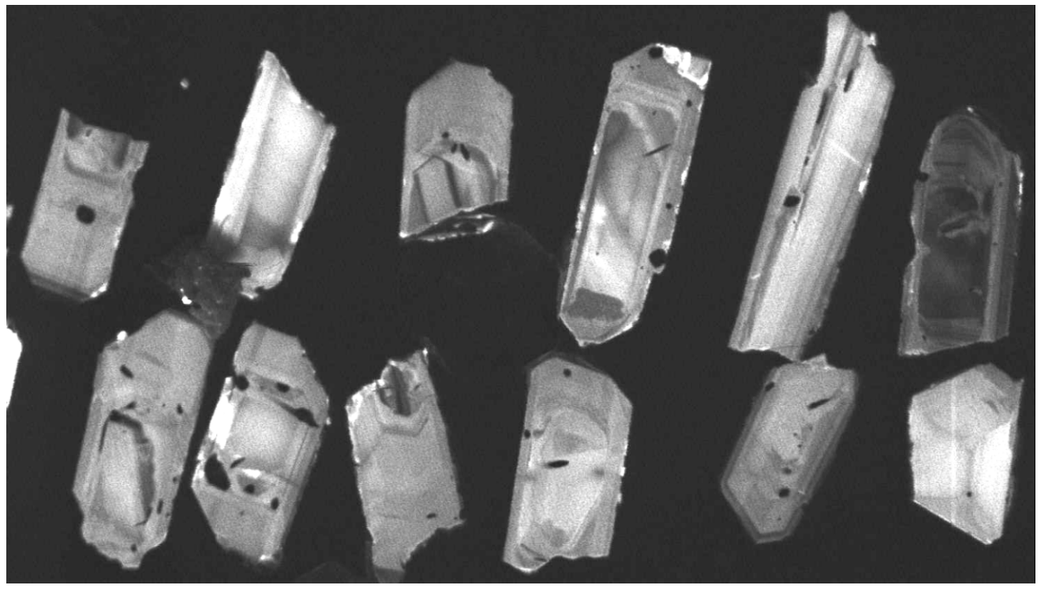

340-1-7A Medium

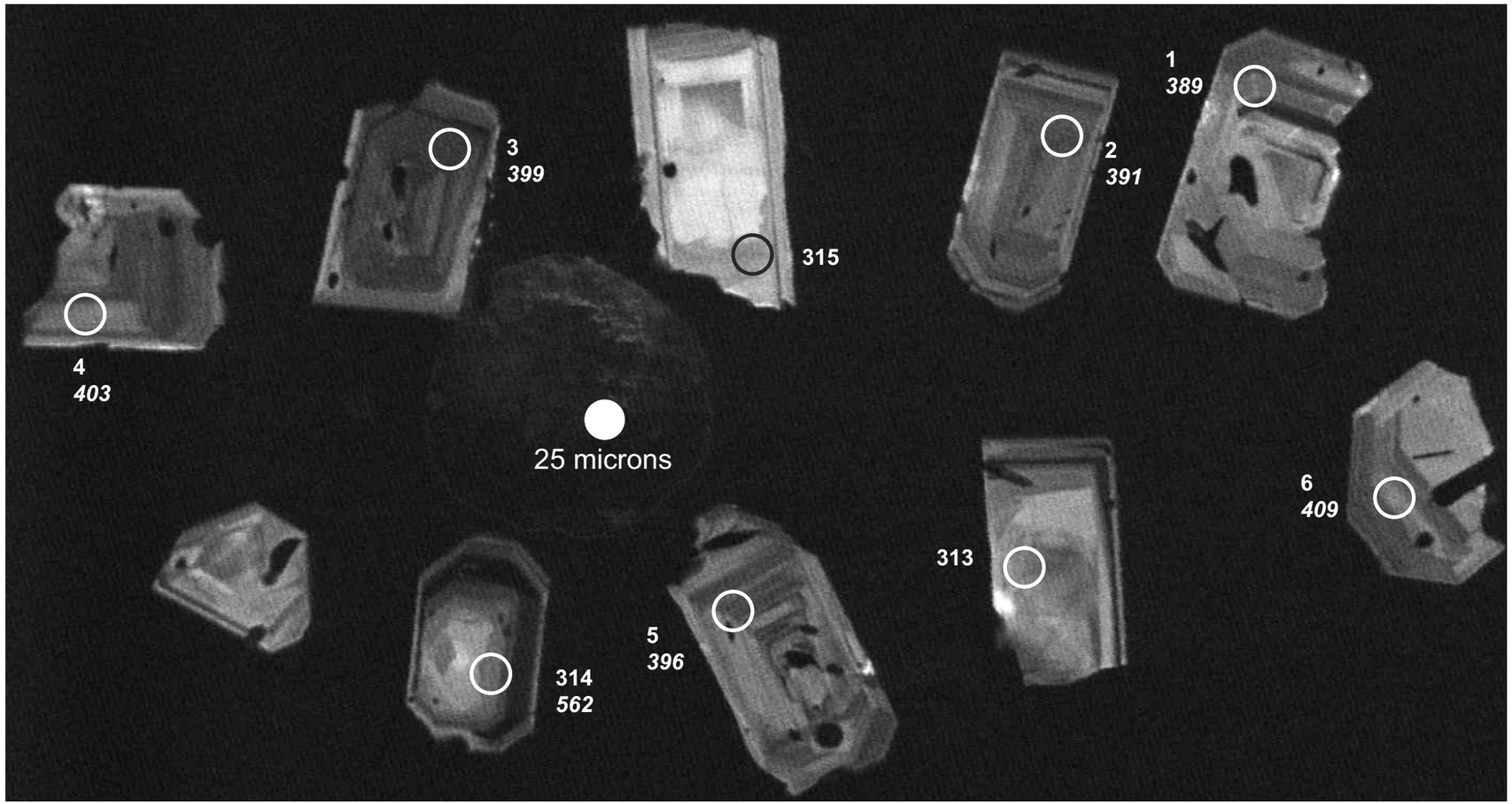

340-1-7A Small

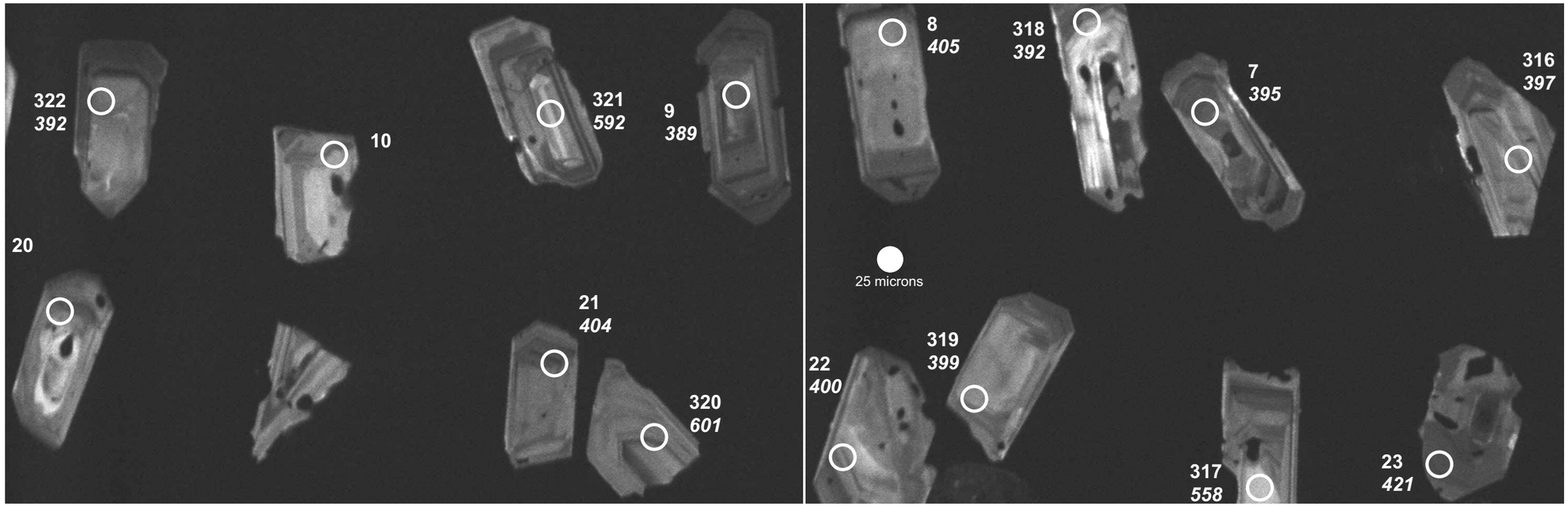

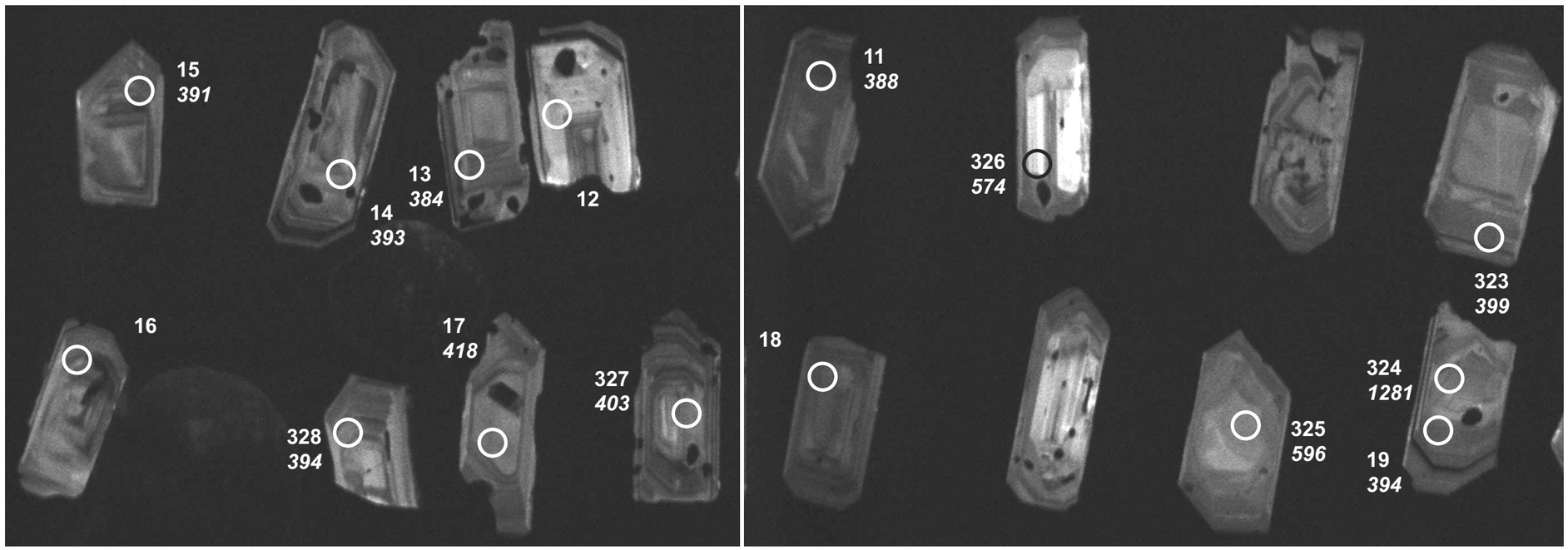

340-1-7A Extra Small

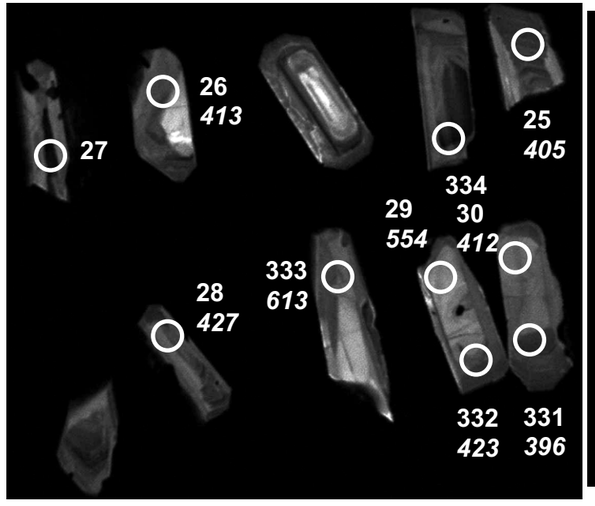

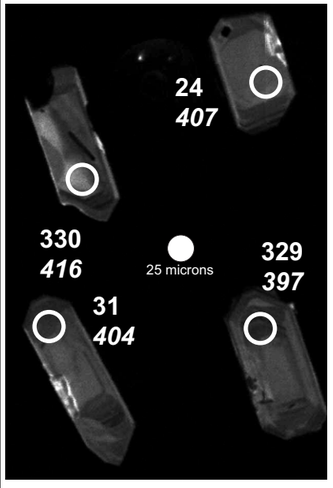

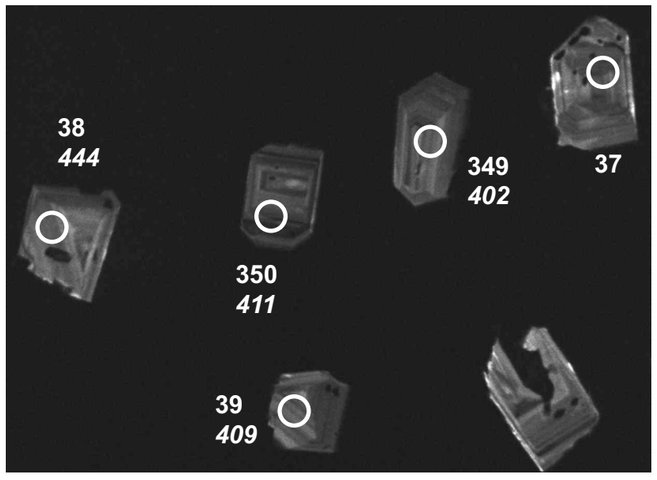

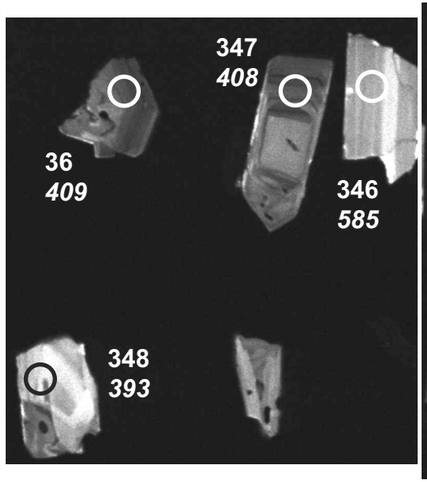

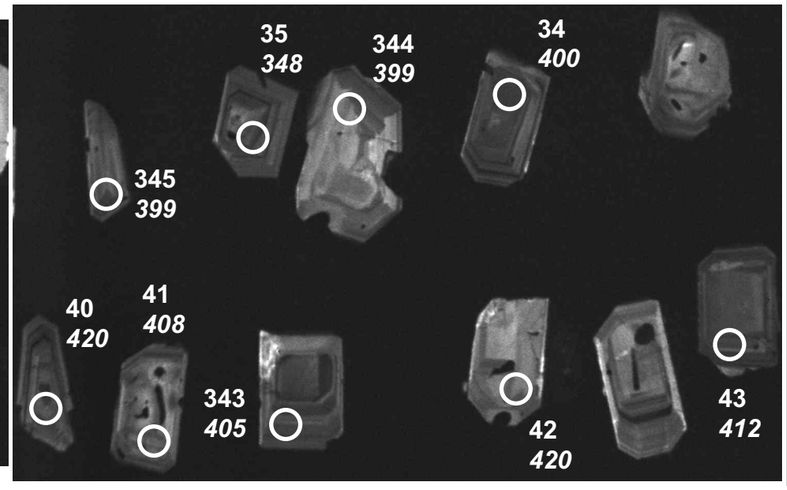

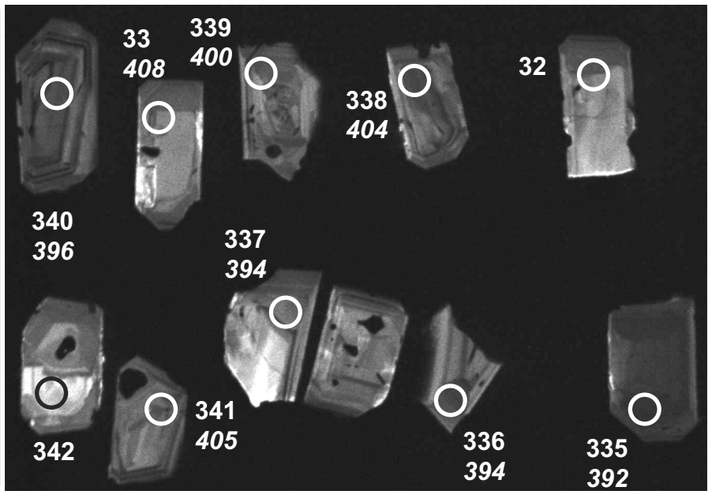

ALV-342-1-1A Large

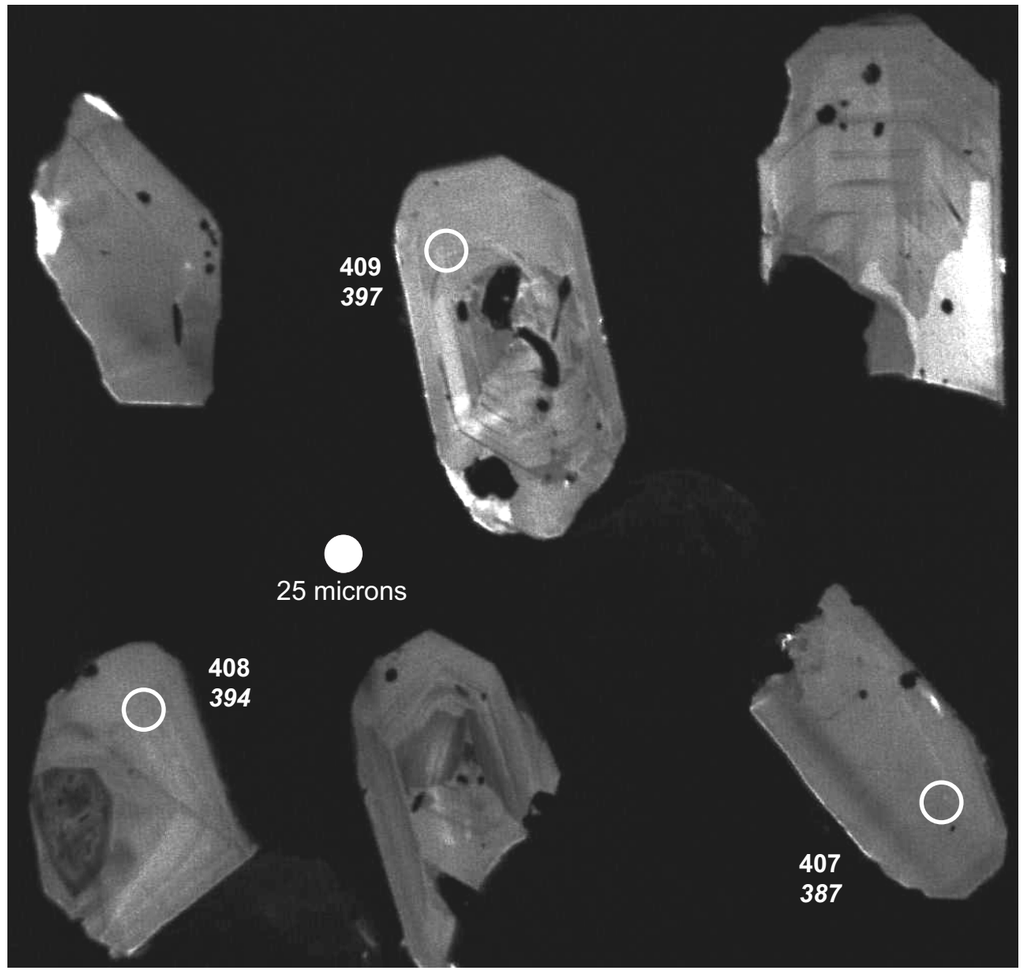

ALV-342-1-1A Medium

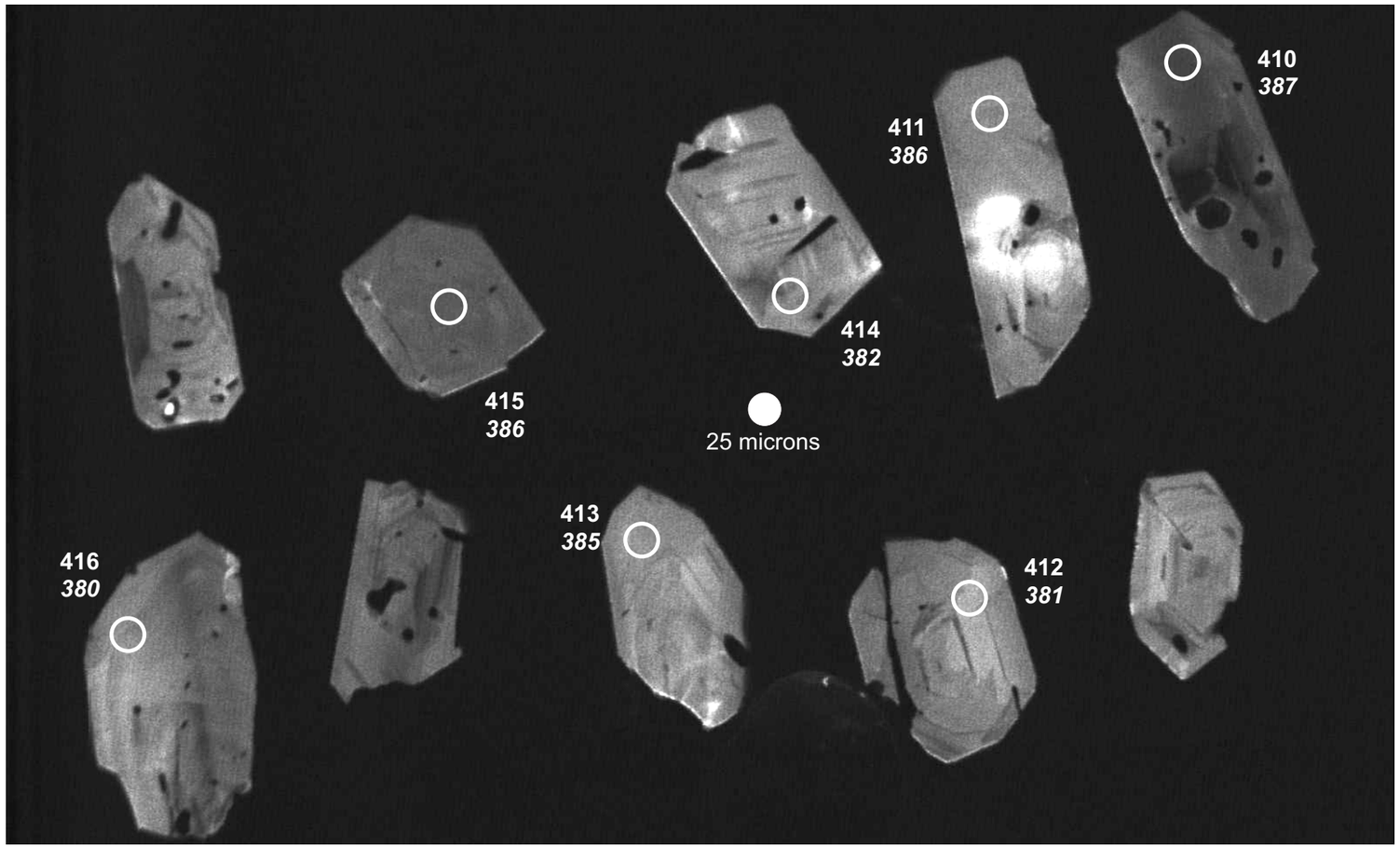

ALV-342-1-1A Small

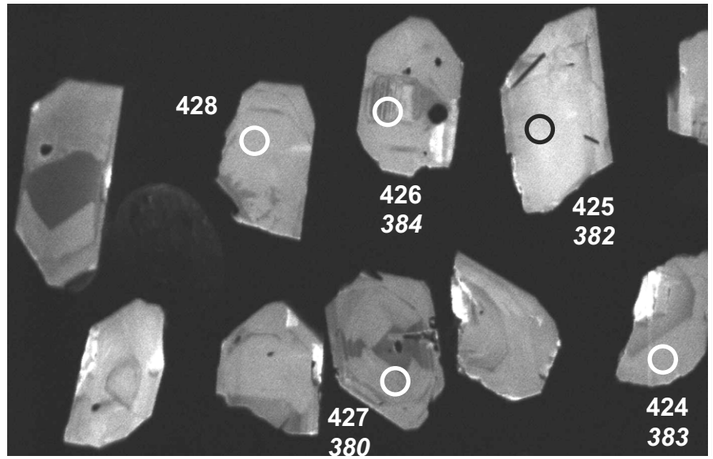

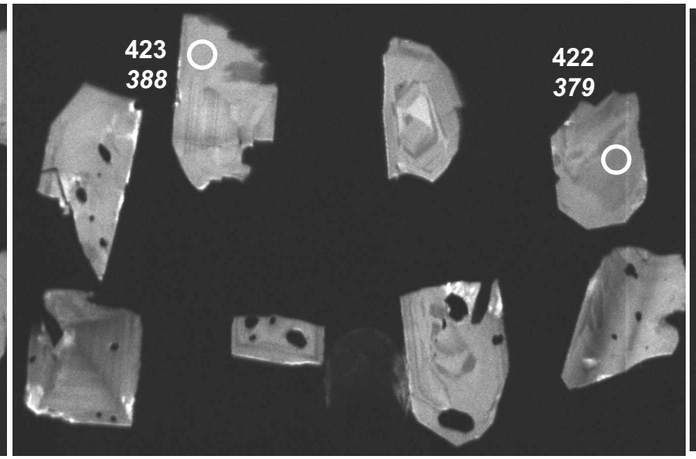

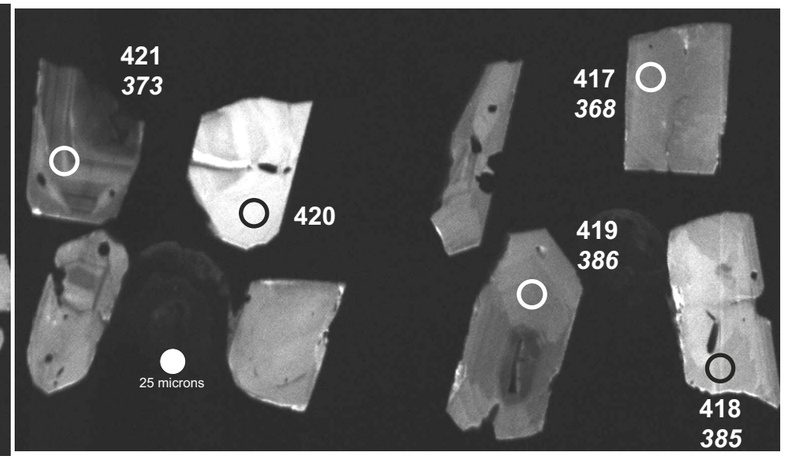

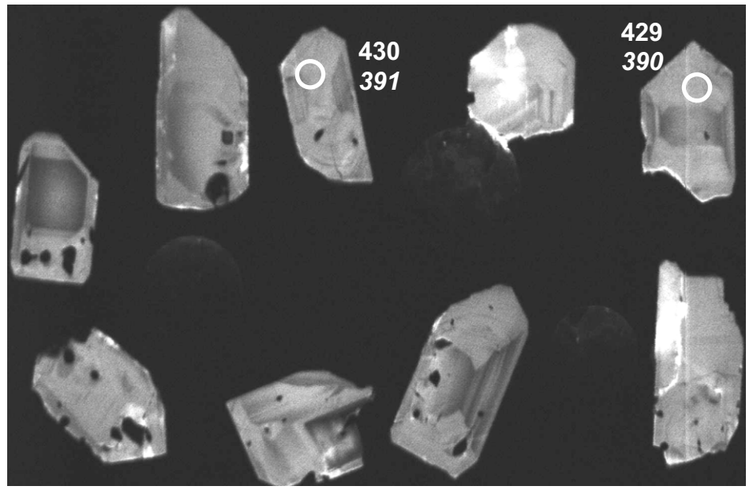

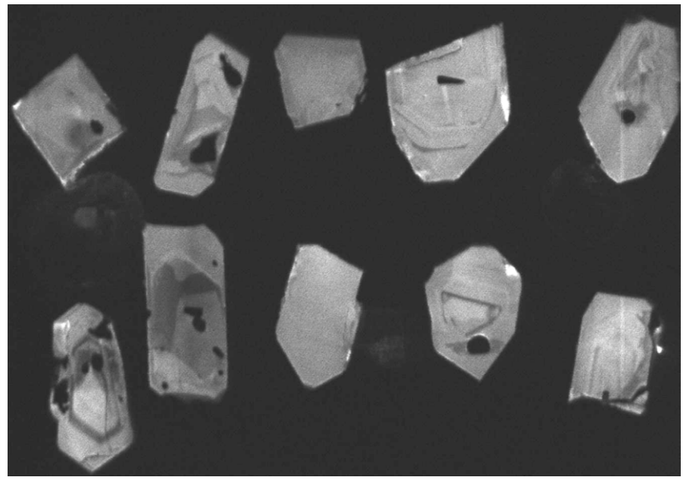

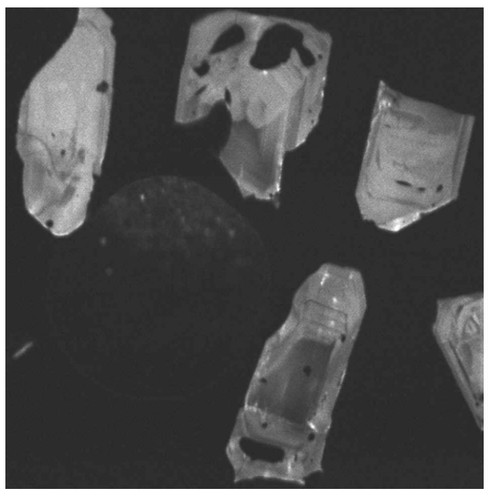

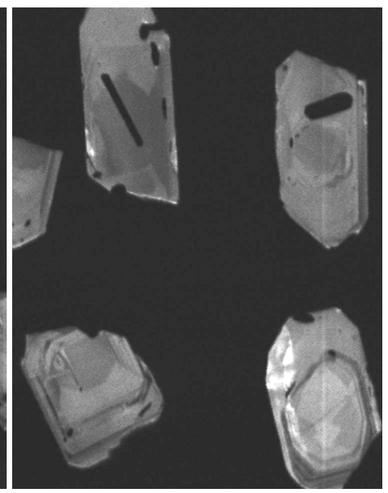

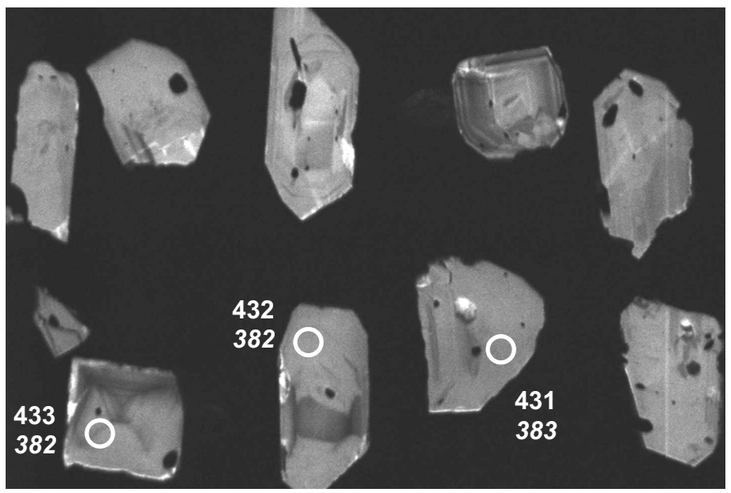

ALV-342-1-1A Extra Small

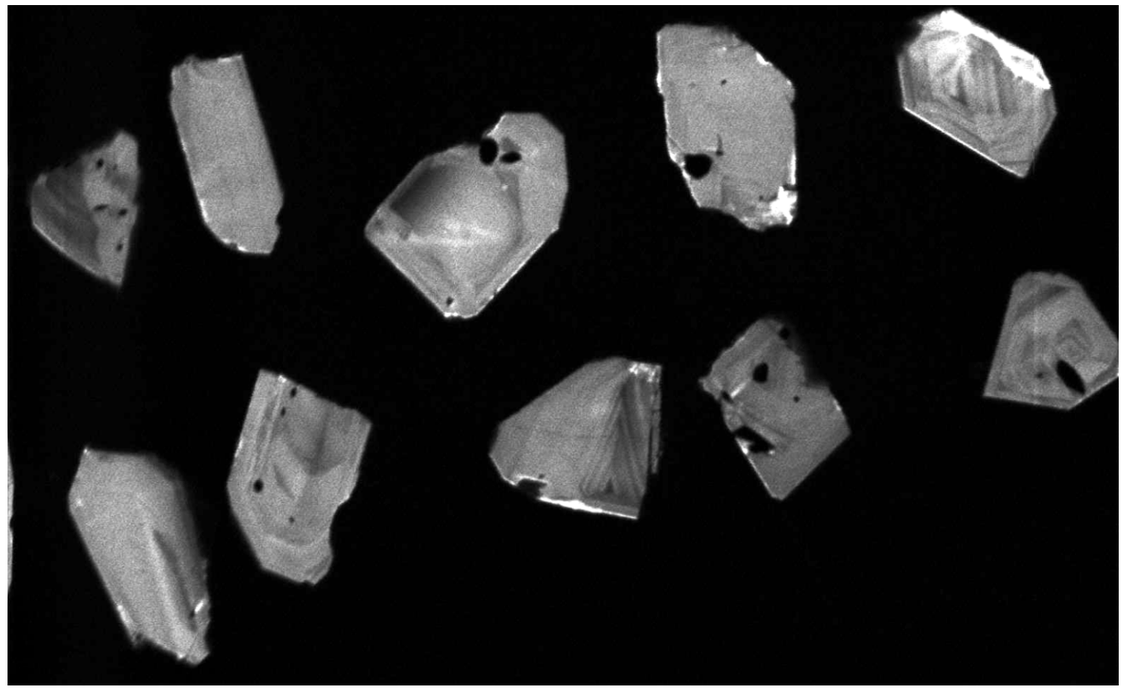

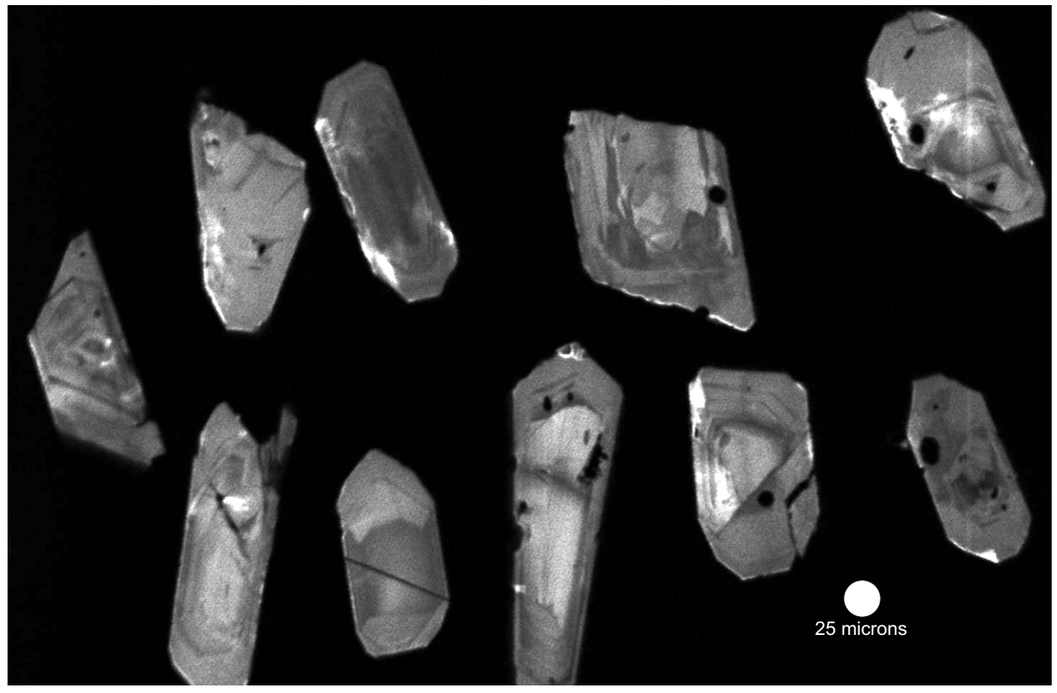

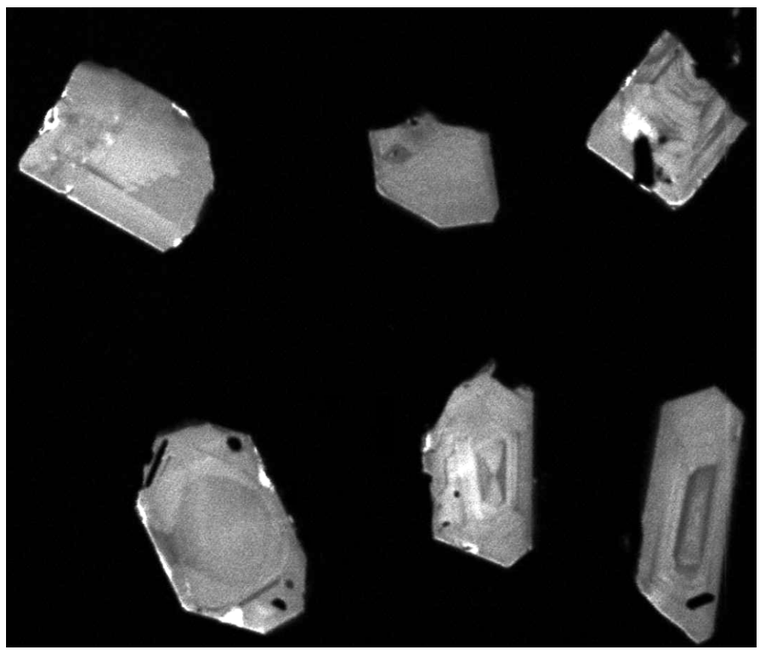

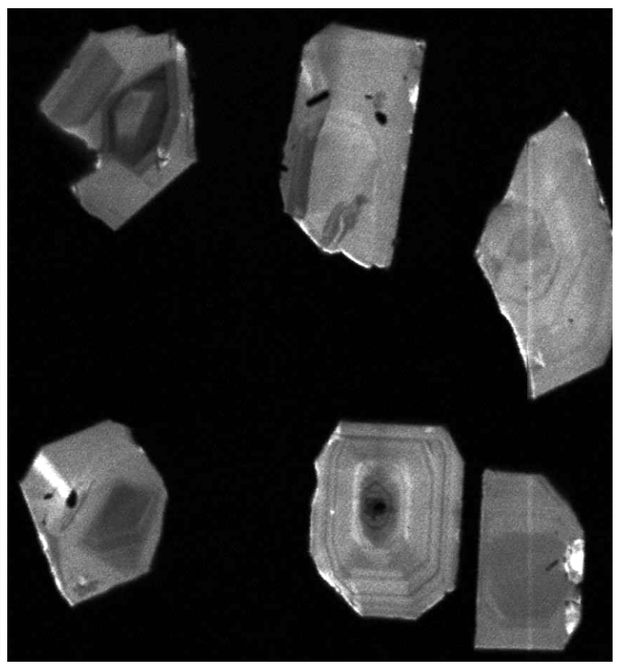

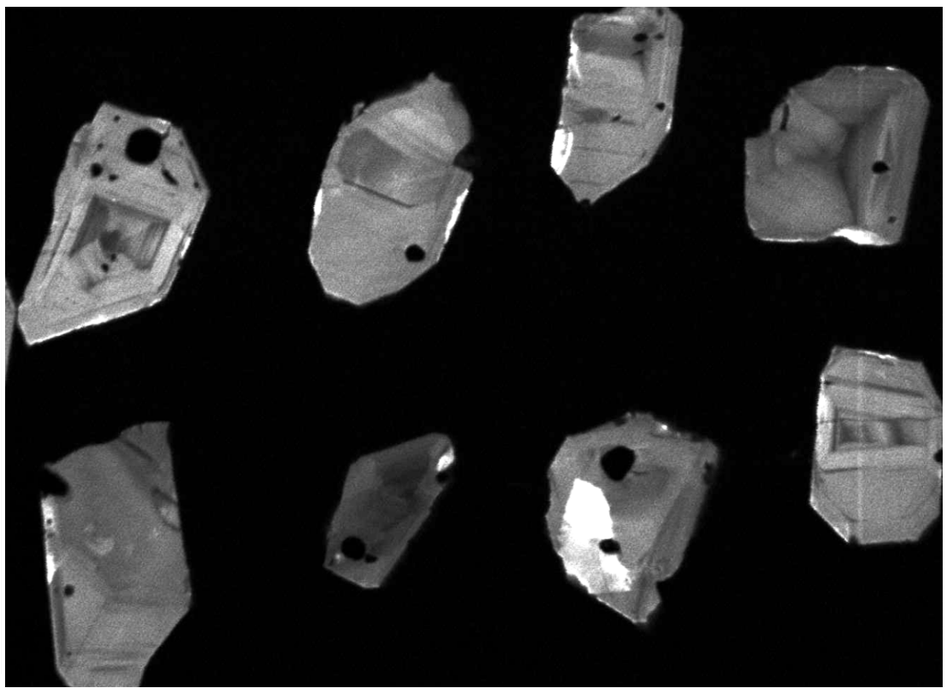

ALV-342-5-3 Large

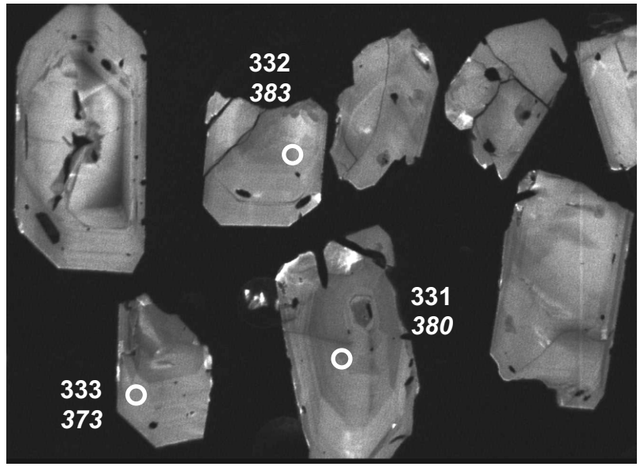

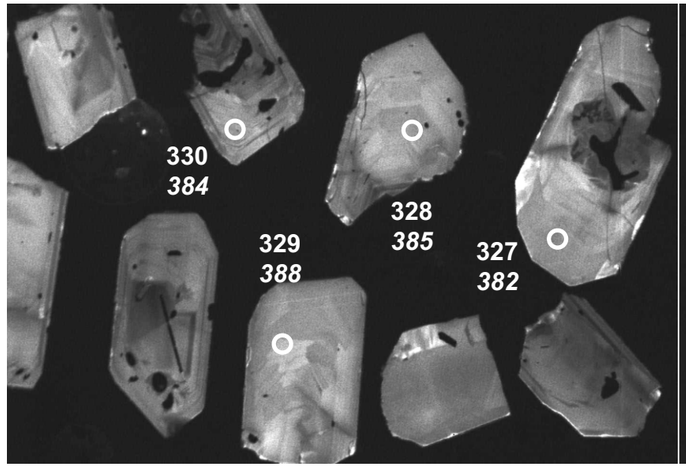

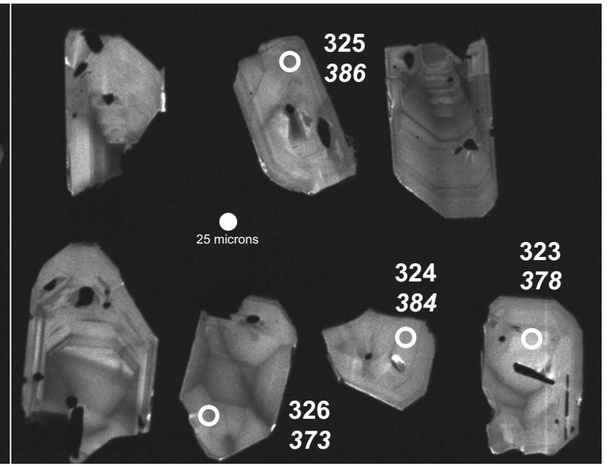

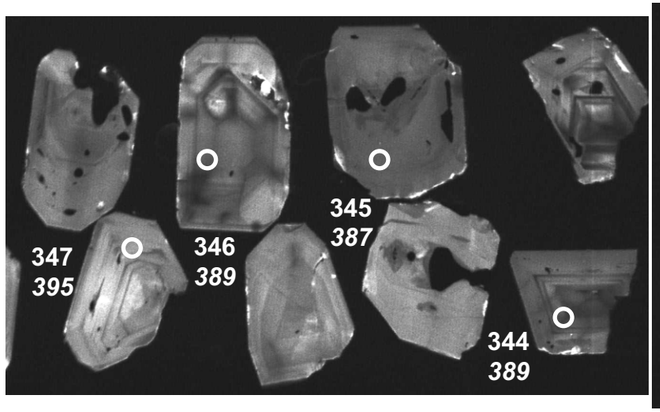

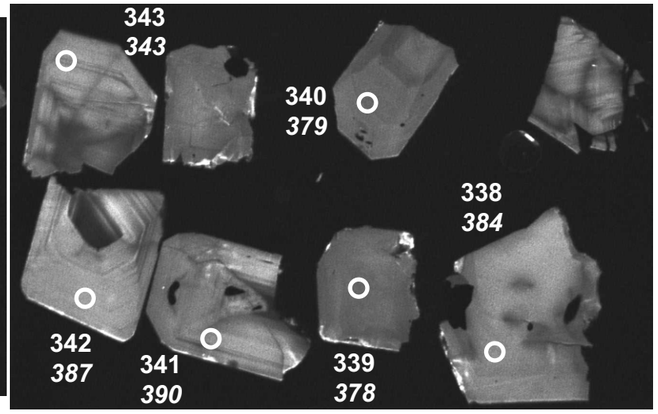

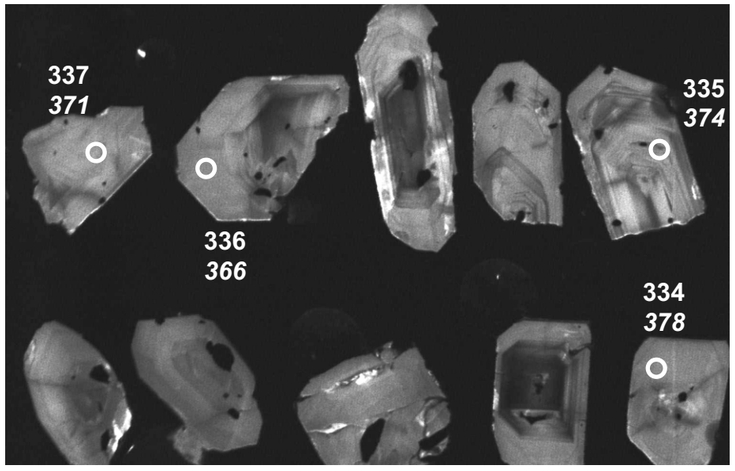

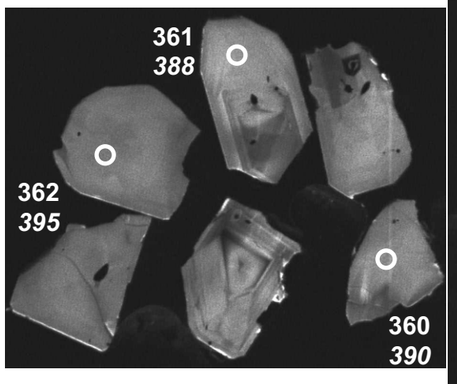

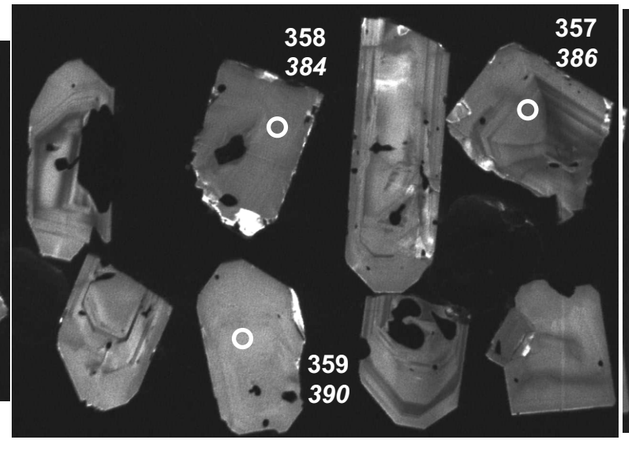

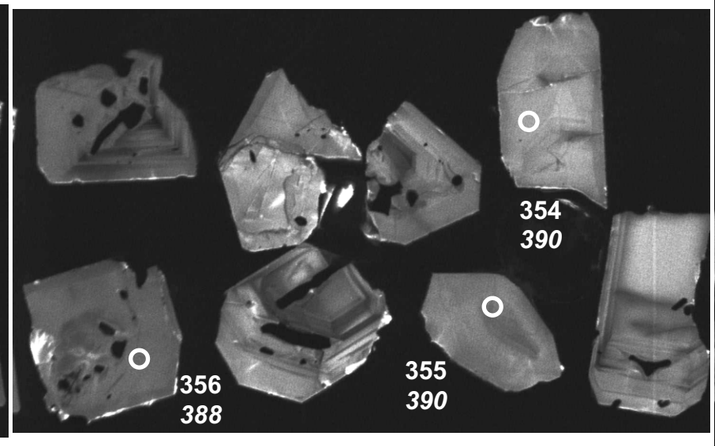

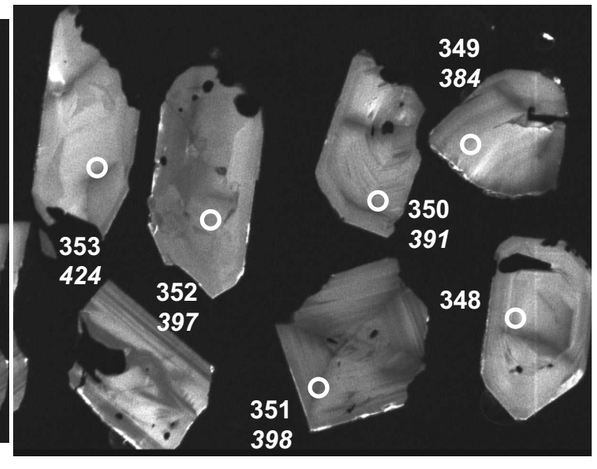

ALV-342-5-3 Medium

APPENDIX

Supplementary data file S1 Tables S2, S3, S4, S5, S6, and S7 are also in open access here: https://doi.org/10.25545/NGMOHK